CFIRE

Title: Corrosion Protection and Steel-Concrete Bond Improvement of Prestressing Strand

CFIRE 05-12
December 2012

National Center for Freight & Infrastructure Research & Education
Department of Civil and Environmental Engineering
College of Engineering
University of Wisconsin–Madison

Authors:
Professors Marc Anderson and Michael Oliva, Dr. M. Isabel Tejedor
University of Wisconsin–Madison

Principal Investigator:
Professor Marc Anderson
National Center for Freight & Infrastructure Research & Education
University of Wisconsin–Madison

Technical Report Documentation Page

1. Report No. CFIRE 05-12	2. Government Accession No.	3. Recipient's Catalog No. **CFDA 20.701**
4. Title and Subtitle Corrosion Protection of Prestressing Strand in Transportation Structures and Strand-Concrete Bond Improvement		5. Report Date December 2012 6. Performing Organization Code
7. Author/s Marc Anderson, Michael Oliva, and Isabel Tejedor		8. Performing Organization Report No. **CFIRE 05-12**
9. Performing Organization Name and Address National Center for Freight and Infrastructure Research and Education (CFIRE) University of Wisconsin-Madison 1415 Engineering Drive, 2205 EH Madison, WI 53706		10. Work Unit No. (TRAIS) 11. Contract or Grant No. **DTRT06-G-0020**
12. Sponsoring Organization Name and Address Research and Innovative Technology Administration U.S. Department of Transportation 1200 New Jersey Ave, SE Washington, D.C. 20590		13. Type of Report and Period Covered **Final Report [10/1/2011 – 9/30/2012]** 14. Sponsoring Agency Code
15. Supplementary Notes **Project completed for USDOT's RITA by CFIRE.**		

Corrosion can lead to the premature deterioration and failure of transportation structures. In pre-stressed bridge structures corrosion is more severe, leading to sudden failures when cracking is induced at pitting sites by tensile or compressive stresses. This work studies the viability and effectiveness of inorganic nanoporous coatings as corrosion protection for carbon steel prestressing strand. Inorganic nanoporous metallic coatings can offer the benefit of not reducing, but possibly enhancing the steel-concrete bond and adding some corrosion resistance to the strand. Anodic Polarization measurements of critical pitting corrosion potential were performed on Grade 270 low-relaxation steel wires from three strand manufacturers in bare and coated conditions. In addition, the wires were subjected to tensile stresses as they would be on a prestressing application and subsequently tested for pitting corrosion potential. Two metallic oxide coatings were used in this work namely acidic zirconia (ZrO_2) and acidic titania (TiO_2). The steel-concrete bond characteristics were measured by pull-out tests based on the current NASP Bond Test Research. Finally, tension tests measure the elastic modulus and strength of the steel before and after the heat treatment involved the coating process. Findings show an increase in corrosion resistance of coated wires prior to being stressed in tension. After tensioning the wires to 80% of their ultimate capacity, the corrosion resistance generally decreases. Pull-out tests show a 100-150% increase of bond strength for coated wires. No effects on the mechanical properties of the steel can be appreciated for heated treated samples with respect to those that have not been heated.

17. Key Words Corrosion, Steel Strand, inorganic oxide coatings, Pull-Out Force.	18. Distribution Statement **No restrictions. This report is available through the Transportation Research Information Services of the National Transportation Library.**		
19. Security Classification (of this report) **Unclassified**	20. Security Classification (of this page) **Unclassified**	21. No. Of Pages	22. Price **-0-**

Form DOT F 1700.7 (8-72) **Reproduction of form and completed page is authorized.**

DISCLAIMER

This research was funded by the National Center for Freight and Infrastructure Research and Education. The contents of this report reflect the views of the authors, who are responsible for the facts and the accuracy of the information presented herein. This document is disseminated under the sponsorship of the Department of Transportation, University Transportation Centers Program, in the interest of information exchange. The U.S. Government assumes no liability for the contents or use thereof. The contents do not necessarily reflect the official views of the National Center for Freight and Infrastructure Research and Education, the University of Wisconsin, the Wisconsin Department of Transportation, or the USDOT's RITA at the time of publication.

Executive Summary

Corrosion Protection of Prestressing Strand in Transportation Structures and Strand-Concrete Bond Improvement

Project Summary:

This work has been devoted to the viability and effectiveness of inorganic nanoporous coatings as corrosion protection for carbon steel prestressing strand. Inorganic nanoporous metallic coatings can offer the benefit of not reducing, but possibly enhancing the steel-concrete bond and adding some corrosion resistance to the strand. Two metallic oxide coatings were used in this work namely acidic zirconia (ZrO_2) and acidic titania (TiO_2). Our findings have shown an increase in corrosion resistance of coated wires prior to being stressed in tension. Pull-out tests show a 100-150% increase of bond strength for coated wires. It would appear that these coatings could be effectively applied in a commercial fashion for mitigating corrosion and increasing strand-concrete bond strength in prestressing strand.

Background:

The useful life of prestressed concrete members in transportation structures can be seriously affected by deterioration due to corrosion of the steel strand. This is more severe in bridge structures close to marine environments where seawater is present and in cold regions where de-icing salts are used during the winter period since pre-tensioned members use uncoated strands or bars. The loss of even one or a few strands has a great impact on prestressed members since their ability to sustain load relies on the tensile strength of the tendons. Weakening of the steel and resultant concrete cracking causes loss of prestress transfer and failure of the member.

Corrosion is a complex phenomenon related to structural, physical, chemical and environmental considerations. The cement paste in concrete provides an alkaline environment that protects the steel from general corrosion. However, corrosion of reinforcing steel in concrete structures, when exposed to chlorides, is a common occurrence. Not only does this process affect the mechanical properties and behavior of the steel reinforcing but also the composite behavior of

the prestressed member.

The ability of a prestressed girder, for example, to sustain service loads and control cracking lies in the attained transfer lengths. The latter term refers to the length through which the initial prestress is effectively transferred to the concrete. This length is in turn dependant on the bond strength of the steel tendon to the concrete. The nature of bond strength is complex and relies on chemical adhesion, friction, mechanical interlock and varies throughout the length of the member.

In addition to safety concerns of highway bridges and other prestressed structures, the cost of corrosion is a major problem. The annual direct cost of corrosion in highway bridges in the United States is estimated at $8.3 billion [2] including replacement and maintenance. The deteriorating effects and high costs of corrosion on pre-stressed concrete members have led to the development of a number of corrosion protection methods. The most common approaches are: concrete sealers and barriers, chemical stabilization, electrochemical protection, and steel coating. However, these methods are not without flaws and their use is limited.

A new corrosion protection method that does not decrease the steel-concrete bond has been investigated in this work. These studies take advantage of previous studies involving the use of novel nanoporous inorganic coatings as developed at the Water Chemistry and Technology Laboratory at the University of Wisconsin. These coatings should provide adequate protection and be thin enough to not affect bonding and may, on the contrary, add some adhesion to cement. To the best of our knowledge this is the first time these nanoporous coatings have been used on steel strand for the prevention of corrosion and is therefore a “first-of-its-kind” research project.

While this project has been performed at the University of Wisconsin in Madison, three companies that manufacture strand have donated materials to this project. The companies also have been kept abreast of our findings and indeed represent possible users of this technology.

Process:

This work has concentrated on two main objectives; assessing the corrosion resistance of coated strand and studying the effect of the coating on bond strength. The corrosion resistance of bare and coated wires was tested by electrochemical methods specifically anodic polarization. From this technique the corrosion pitting potential of the sample was obtained and corrosion rates were qualitatively compared to strand not coated. For the second objective, we determined the steel-concrete bond of both bare and coated samples for Grade 270 strand of 0.5in and 0.6in diameter. The steel-concrete bond strength was evaluated by small-scale pull-out tests based on the North American Strand Producers (NASP) Bond Test developed for the National Cooperative Highway Research Program (NCHRP) 603 Report.

Many Samples of three different types of strand were cleaned and coated followed by firing the coatings at 350^0C in an air atmosphere after which electrochemical studies were performed in the Environmental Chemistry and Technology Program – UW Madison. These tests were compared with control samples run on these same strand samples without the nanoporous coatings. Pull-out tests were conducted in the Highway Lab at the UW Madison. These consisted of pouring concrete around embedded strand and then subjecting this strand to the forces required to dislodge the strand from the hardened concrete.

Findings and Conclusions:

The quality of the coating is affected largely in part by the condition of the substrate, in this case the carbon steel surface. Treating the wires with either acid solutions of HNO_3 or HCl or a basic solution of 1:4 ratio of H_2O_2 and 3M NaOH improves the nature of the oxide films and the protection of these coatings against corrosion. The basic treatment was the most effective.
Wires coated with zirconia render more positive critical pitting corrosion potentials than the ones coated with titania. Zirconia was subsequently used for all electrochemical and structural testing.
An improvement on the corrosion resistance of a material is analogous to a change in the critical

pitting corrosion potential, E_{pit}, of the material to a more positive value. More positive pitting potential values were recorded for coated samples relative to bare wire, regardless of the manufacturer.

Results from bond testing can be interpreted in two ways. As opposed to the NASP Test and other pull-out tests discussed in the literature, our small-scale test used only one single wire as a test specimen, embedded in concrete mortar. The bond is mainly provided by chemical adhesion and friction since mechanical interlock is negligible. From our small-scale pull-out tests it can be concluded that these nanoporous oxide coatings do significantly improve adhesion to concrete, which will benefit the bond stress.

Recommendations:

While electrochemical testing has indicated that nanoporous oxide coatings improve the corrosion resistance of strand, these results should be complemented with Electrochemical Impedance Spectroscopy (EIS) studies in order to have a better understanding of the processes occurring at the electrode (steel) interface and the type of protection offered by the coatings. More research should be focused on the steel surface characterization and pretreatment. The effectiveness of the coating is sensitive to the condition of the substrate and a significant amount of research time should be allotted to this subject. Also, further testing should include coating the whole strand and testing the coating's resistance to abrasion as well as its electrochemical behavior. Electrochemical testing of coated strands embedded in concrete should also be considered, with careful consideration to variables such as environmental pH, curing temperature

and permeability of the concrete.

In situ electrochemical tests should be performed while the wire or strand is subjected to some tension as it would be on a prestressed concrete girder. If electrochemical testing and SEM photos cannot be taken of stretched wire, one should consider removing the stress at a very slow rate so as to avoid fast, drastic changes in microstructure. Finally, in terms of its effect on the steel-concrete bond, a full NASP bond test should be performed and compared to the literature.

From a policy point of view, it would appear that these coatings not only provide corrosion resistance for strand but bond strength might also be improved if companies would fabricate their strand with the coatings. The amount of material required to coat strand is very small as the layer thickness is only 0.2 microns. It would seem that this could provide some company a favorable market edge if they were to implement this technology.

Corrosion Protection of Prestressing Strand in Transportation Structures and Strand-Concrete Bond Improvement

by

Carla S. Príncipe-Martínez

A thesis submitted in partial fulfillment of

the requirements for the degree of

Master of Science

Civil Engineering

At the University of Wisconsin - Madison

Dr. Michael Oliva

Dr. Marc A. Anderson

Dr. Isabel Tejedor

Corrosion Protection of Prestressing Strand in Transportation Structures and Strand-Concrete Bond Improvement

Carla S. Príncipe-Martínez

Abstract

Corrosion can lead to the premature deterioration and failure of transportation structures. In pre-stressed bridge structures corrosion is more severe, leading to sudden failures when cracking is induced at pitting sites by tensile or compressive stresses. This work studies the viability and effectiveness of inorganic nanoporous coatings as corrosion protection for carbon steel prestressing strand. Inorganic nanoporous metallic coatings can offer the benefit of not reducing, but possibly enhancing the steel-concrete bond and adding some corrosion resistance to the strand. Anodic Polarization measurements of critical pitting corrosion potential were performed on Grade 270 low-relaxation steel wires from three strand manufacturers in bare and coated conditions. In addition, the wires were subjected to tensile stresses as they would be on a prestressing application and subsequently tested for pitting corrosion potential. Two metallic oxide coatings were used in this work namely acidic zirconia (ZrO_2) and acidic titania (TiO_2). The steel-concrete bond characteristics were measured by pull-out tests based on the current NASP Bond Test Research. Finally, tension tests measure the elastic modulus and strength of the steel before and after the heat treatment involved the coating process. Findings show an increase in corrosion resistance of coated wires prior to being stressed in tension. After tensioning the wires to 80% of their ultimate capacity, the corrosion resistance generally decreases. Pull-out tests show a 100-150%

increase of bond strength for coated wires. No effects on the mechanical properties of the steel can be appreciated for heated treated samples with respect to those that have not been heated.

Acknowledgements

First I would like to acknowledge the support of the National Center for Freight and Infrastructure Research and Education (CFIRE). This project was funded by CFIRE to test the ability of inorganic nanoporous coating developed in the University of Wisconsin to be use as a method for corrosion protection of prestressing tendons used in transportation structures.

I would like to offer my special thanks to Dr. Isabel Tejedor for her mentorship and assistance in the interpretation of anodic polarization and energy dispersive spectroscopy data and for help throughout the completion of this work. To Professor Michael Oliva, Professor Marc Anderson and graduate students Jessica Sanfilippo and Jennifer Jackowski, I would also like to extend my thanks for their mentorship on this project.

I would also like to acknowledge undergraduate student Kyle Busch for his help in the initial stages of the project and his vital help during the tension testing portion of this work. I would also like to extend my appreciation to engineer Matt Badman from the Sumiden PC Strand Division for his time and providing information on strand manufacturing and the mechanical properties and specs of the reel of strand donated for the project.

Lastly, I would like to thank my family, my mom and dad whose influence on my education and academic successes are undeniable. Also, I thank my sister for her support, her companionship and her unwavering belief in my ability.

Table of Contents

List of Figures

List of Tables

Chapter 1: Introduction

1.1 Problem Statement Summary

The useful life of prestressed concrete members in transportation structures can be seriously affected by deterioration due to corrosion of the steel strand. This is more severe in bridge structures close to marine environments where seawater is present and in cold regions where de-icing salts are used during the winter period since pre-tensioned members use uncoated strands or bars [1]. Also, aggregate chloride contamination can be a factor leading to corrosion of the strand.

The loss of even one or a few strands has a great impact on prestressed members since their ability to sustain load relies on the tensile strength of the tendons. Weakening of the steel and resultant concrete cracking causes loss of prestress transfer and failure of the member. For example the girder in Figure 1.1 shows clear signs of concrete spalling caused by the corrosion products of rusting strand in the US-45 Bridge in Milwaukee.

Figure-1. 1 Strand and rebar deterioration in US 45 bridge in Milwaukee

Corrosion is a complex phenomenon related to structural, physical, chemical and environmental considerations. The cement paste in concrete provides an alkaline environment that protects the steel from general corrosion. However, corrosion of reinforcing steel in concrete structures, when exposed to chlorides, is a common occurrence. Not only does this process affect the mechanical properties and behavior of the steel reinforcing but also the composite behavior of the prestressed member.

The ability of a prestressed girder, for example, to sustain service loads and control cracking lies in the attained transfer lengths. The latter term refers to the length through which the initial prestress is effectively transferred to the concrete. This length is in turn dependant on the bond strength of the steel tendon to the concrete. The nature of bond strength is complex and relies on chemical adhesion, friction, mechanical interlock and varies throughout the length of the member. Because of the complexity and importance of the steel-concrete bond many researchers and agencies have developed several methods for predicting bond. The North American Strand Producers (NASP) Bond Test is one of the most studied methods and has been compared to other methods such as the Moustafa Method and found to be more repeatable. This method has been studied in many universities such as the University of Oklahoma and Purdue University in a series of "round robin" tests. While there is no current standard test for bond strength this method has been used in previous works to assess the bond characteristics and performance of steel prestressing strand.

In addition to safety concerns of highway bridges and other prestressed structures, the cost of corrosion is a major problem. The annual direct cost of corrosion in highway bridges in the United States is estimated at $8.3 billion [2] including replacement and maintenance. The

deteriorating effects and high costs of corrosion on pre-stressed concrete members have led to the development of a number of corrosion protection methods. However, these methods are not without flaws and their use is limited. There are several corrosion protection strategies available. The most common approaches are: concrete sealers and barriers, chemical stabilization, electrochemical protection, and steel coating. An ultimate alternative is to replace the steel with materials such as stainless steel or fiber-reinforced plastic.

Concrete surface sealers and barriers function by providing an impervious layer on or in the concrete between corrosives agents and the steel. The typical procedure is to use overlays composed of latex-modified concrete, low-slump concrete, or polymer concrete. Many authors have reported earlier that the chloride-induced corrosion of steel reinforcement can be effectively controlled by the use of a mineral admixture in concrete such as silica fume [3]. However, there are very few studies on the long-term durability of the concrete with micro-silica when exposed to various aggressive environments. In addition, corrosion caused by chloride already in the concrete from contaminated aggregate or concrete additives can still occur. Increasing the concrete depth has proven effective in slowing the ingress of chloride to the steel but is has cost and design limitations.

Chemical protection using migrating corrosion inhibitors (MCI) relies on changing the concrete environment to reduce corrosion. Calcium nitrite, the most commonly used inhibitor, does not reduce the permeability of the concrete, nor does it prevent corrosion. Rather, it competes with chloride to react with the steel and reduce the corrosion rate. Two drawbacks are that it acts as a set accelerator for concrete, and normally needs a retarder.

Second, the amount required is difficult to predict because exposure varies in different parts of the structure.

Cathodic protection works by imposing an electric potential to oppose the corrosion cell. It requires an anode current distribution system and a power supply. The major drawback is that it is a technically sophisticated, expensive system that requires trained-engineer site visits [4]. It also requires high maintenance expenditures and an external power supply, often in remote areas.

Galvanizing provides protection through a zinc barrier between the steel and the environment and by the Zn acting as a sacrificial anode for the steel. Observations from a seawater exposure evaluation showed clear evidence of progressive corrosion of the zinc layer under natural exposure conditions but the volume of the corrosion products is often less than that of iron products. The main drawback of this technique is the need for a sacrificial material, Zn, and thus, the protection will last only as long as the Zn is still present [5]. In addition the Zn ions will contaminate the environment.

Epoxy-coated reinforcement (ECR) is used extensively in construction to protect steel from corrosion. Epoxy coating works by preventing chloride and moisture from reaching the surface of the steel. Some studies have shown favorable results, while other research has documented poor performance. In a study by Clear, he found that ECR typically outperformed uncoated reinforcement, but the increased performance was not long term. Clear determined that on epoxy coated rebar the increase in life of ECR in northern U.S. and Canadian environments would be in the range of only 3 to 6 years in most instances, rather

than the more than 40 years previously estimated [6]. This was attributed to the progressive loss of coating adhesion to the steel and under-film corrosion.

A new corrosion protection method that does not decrease the steel-concrete bond is proposed in this work. The use of novel nanoporous inorganic coatings has been tested at the Water Chemistry and Technology Laboratory at the University of Wisconsin on stainless steels. These coatings should provide adequate protection and be thin enough to not affect bonding and may, on the contrary, add some adhesion to cement.

1.2 Objectives

This research study was funded by the National Center for Freight and Infrastructure Research and Education (CFIRE) to determine the viability of inorganic nanoporous coatings for improving the corrosion resistance of steel prestressing strand while preserving or possibly enhancing the steel-concrete bond. This paper will focus on two main objectives; assessing the corrosion resistance of coated strand and the effect of the coating on bond strength.

Corrosion Resistance: The first objective is to improve the resistance to corrosion of the steel strand with the use of inorganic nanoporous coatings. The corrosion resistance of bare and coated wires was tested by electrochemical methods specifically anodic polarization. From this technique the corrosion pitting potential of the sample was obtained and corrosion rates were qualitatively compared.

Coating Adhesion: In order to obtain a quality coating and accomplish the first objective, the substrate must be studied and pretreated in the same fashion as that used to apply the coating. An additional objective of the research was to identify the composition of the steel surface and find a pretreatment that improves the adhesion of the coating to the steel.

Bond Strength: The second main objective of this research is to determine the steel-concrete bond of both bare and coated samples for Grade 270 strand of 0.5in and 0.6in diameter. The quality of the bond is of major significance in the mechanics of stress transfer and its relationship to the transfer lengths of strand in prestressed concrete members. The steel-concrete bond strength was evaluated by small-scale pull-out tests based on the North American Strand Producers (NASP) Bond Test developed for the National Cooperative Highway Research Program (NCHRP) 603 Report. The test was not compared to any publication but served to compare the bond behavior of bare and coated wire embedded in mortar cylinders. In this manner a positive, negative or neutral effect of the coating to the bond quality can be verified.

Mechanical Properties: Additionally, in order to assess the viability of the coating procedures, tension tests have been included as part of this work. Mechanical properties of the strand in as-received condition such as ultimate tensile strength, breaking strength and modulus of elasticity, are quantified and compared to those of strand that have been subjected to the heat treatments involved in the coating process.

1.3 Proposed Solution

A new type of corrosion protection for pre-stressing steel strand is introduced. The research presented in this report seeks to determine the viability and effectiveness of novel nanoporous inorganic coatings as a corrosion protection method for steel prestressing strand with no reduction in steel-concrete bond. This is the first phase in adapting this material to prestressing applications. The method of applying the coating, added corrosion protection and bond to concrete has been examined and is discussed in the following chapters.

1.2.1 Nanoporous Inorganic Coatings

The coatings used for this project are applied to the substrate by sol-gel deposition and consist of metallic oxide nanoparticles in acidic colloidal suspensions that, by sintering, form an integrated network of discrete nanoparticles. The finished coating is a ceramic material.

Initial corrosion studies using inorganic nanoporous coatings have been carried out by the Department of Environmental Chemistry and Technology at the University of Wisconsin-Madison. These coatings were prepared by dip-coating stainless steel plates into suspensions containing TiO_2 or ZrO_2 nanoparticles. Initial findings indicated an increase of corrosion potential for coated stainless plates than uncoated plates. Differences in electric potential between coated and uncoated plates can be as large as 0.5V. The higher the voltage sustained before the current increases, the greater the corrosion resistance. Both ZrO_2 and TiO_2 coatings showed significant improvements in corrosion resistance and were therefore chosen for this project.

1.4 Scope of Work

This work focuses on the determining how viable inorganic nanoporous coatings are for corrosion protection use. The desired surface condition for the steel was determined and treatments have been suggested to prepare the steel surface for coating. Two coatings were tested, zirconia (ZrO_2) and titania (TiO_2) of which the one offering the better corrosion protection was used for structural tests. Appropriate coating thickness, as number of coating layers, was also determined.

The effect of the coating on the steel-concrete bond was quantified by a small-scale version of the bond test proposed by the NASP Association in conjunction with the University of Oklahoma.

About 36ft of strand was donated by each of the three manufacturers: Sumiden, Insteel and American Spring Wire. For simplicity and due to limited amount of material all testing was done on single wires. This requires that the bond test be modified from the method described in the NASP Round IV Bond Test.

The heating procedure used during coating process also requires that some mechanical properties of the steel wires be tested. This was done through tension tests from which the modulus of elasticity, fracture strength and ultimate tensile strength were acquired.

Limitations of the study include the following:

- Electrochemical testing does not take into account the effect of concrete permeability, and degree of concrete cracking due to steel degradation.

- Lack of a bond test standard and modification of the current bond test research procedures to use single wires.
- Inability to currently test the wire for critical pitting corrosion potential and corrosion resistance under applied tension.

1.5 Thesis Organization

This thesis is divided into seven chapters. Chapter 1 introduces the subject and the project objectives and scope. Chapter 2 is a literature review of the corrosion protection methods and bond test procedures. A brief introduction to corrosion mechanisms, electrochemical testing and general information of strand manufacture is presented in Chapter 3. Chapter 4 describes the methodology and results for various steel surface treatments to enhance coating adhesion and quality. Chapter 5, 6 and 7 detail the procedure, test setup and results for the anodic polarization measurements, bond tests and tension tests respectively. Chapter 8 presents the discussion and conclusions derived from testing as well as recommendations for future work.

Chapter 2: Literature Review

2.1 Corrosion Protection Methods for Reinforcing Steel in Concrete

The durability of steel within concrete relies partly upon the alkalinity of the pore solution retained in the hardened cement paste that binds the aggregate and the rebar. Pore solutions have a pH near 13 and their main constituents are $Ca(OH)_2$ and alkaline hydroxides. At this pH, carbon steel "passivates" in the presence of oxygen by forming a surface layer of iron oxides. The composition of the passive layer depends on the oxygen and pH levels and is mainly composed of Fe_2O_3 oxide more or less hydrated and several kinds of FeO oxides in its inner layer. The thickness of the layer generally ranges from 4 to 8 nm [7]. The steel is unlikely to rust as long as the passivating conditions remain.

Well compacted concrete provides a physical diffusion barrier against corrosion by reducing the penetration of atmospheric carbon dioxide (CO_2), oxygen and moisture (3 elements that are necessary to initiate and sustain corrosion reactions). The passivation can be destroyed due to a reduction in alkalinity by the entrance of atmospheric carbon dioxide (carbonation) or sulphur dioxide (SO_2) (industrial climates) or by the ingress of the aggressive chloride ions (e.g. from marine environments) or de-icing salts (e.g. on roads). The rust created on the rebar can increase up to 2 times the volume of the steel, creating high internal stresses that lead to eventual cracking of the concrete or even complete destruction of the member.

During the past decades industrialized countries all over the world have tried to protect concrete from cracking in several different ways such as:

1. Making a better compacted concrete by reducing the water cement ratio *w/c*, using water-reducing admixtures, adding permeability reducing admixtures such as fly ash or silica fume, and blast furnace slag [3]. These treatments will delay the arrival of carbonation and chlorides at the level of the steel reinforcement but cannot be regarded as a long term solution for corrosion protection in bridges.

2. Adding organic base corrosion inhibitors as ethanolamine and guanidine, into carbonated concrete [8].

3. Using stainless steel in lieu of conventional black bars can be a good solution to avoid corrosion, however stainless steel is very expensive and difficult to bend [9].

4. Applying a relatively thin zinc surface layer on the rebar, galvanization, by either hot dipping (hot dip galvanization) or painting the rebar with a thin layer of Zn (cold galvanization). Hot galvanization is not a technique easy to implement, it is easier to apply a layer of special Zn paint. Because zinc is anodic to steel, the galvanized coating provides cathodic protection to exposed steel. When zinc and steel are connected in the presence of an electrolyte, the zinc is slowly consumed while the steel is protected. However, in this system Zn is a sacrificial material and thus the cathodic protection of the steel from corrosion continues only until all the zinc in the immediate area is consumed.

5. Epoxy coating the rebar. This coating is intended to serve as a physical barrier preventing chloride ions and other aggressive matter from coming into contact with the steel surface. This is the most widely used form of corrosion protection in the concrete structures in North America and will be discussed in more detail.

2.2 Organic Coatings – Epoxy Coated Reinforcement (ECR)

Several methods are commonly used to protect steel reinforcement from rusting. Galvanized and stainless steel reinforcement, cathodic protection systems, and chemical and mineral corrosion protection systems are previously mentioned, are less common than epoxy-coated reinforcement [1]. In the early 1970's, the National Bureau of Standards sponsored the first large scale program designed to evaluate the applicability of different coatings for reinforcement protection [10]. Throughout the decade, construction of epoxy coated reinforced bridges continued in the United States. No early field assessment of the corrosion protection of epoxy coating could be performed due to the short term exposure of these new bridges. During the late 1980s, the first field corrosion failures of epoxy-coated reinforcing steel were reported [10]. A number of studies and field work have been conducted on epoxy coated reinforcement to determine its effectiveness as a corrosion protection method and its adequacy for use in marine environments [10]. Unfortunately, many of these studies have yielded no relation between the failure of epoxy coating and a specific parameter or location and failures seem random. In many cases, the use of epoxy coatings is not reliable and does not allow for full development of the steel-concrete bond in the case of prestressed structures, leading to problems in design. The American Association of State Highway and Transportation Officials (AASHTO) does not include epoxy coated strand as an acceptable material for use in bridges because of the poor steel-concrete bond [11].

Study by the University of Virginia

Several studies have focused on testing the effectiveness of epoxy coatings and the variables that control its performance. A research project at the University of Virginia by Pyc (1997)

evaluated sustained damage from corrosion of epoxy coated reinforcing steel removed from job sites in three locations. These specimens were evaluated qualitatively for signs of deterioration and debonding. In addition, behavior of epoxy coated steel in comparison to bare steel was tested through an immersion test in various solutions [12]. The test specimens were immersed in a pore solution at 40°C for a period of 7 days and NaCl subsequently added. The solution was aerated with O_2 once a week. The specimens were visually examined after 4 weeks and every 2 weeks for a period of 90 days for initiation and progress of corrosion[12]. Corrosion can initiate in small areas where the coating has been damaged or has de-bonded. Therefore number of blisters on each specimen was recorded. Hardness of the epoxy coating was tested by "film hardness pencil test" and adhesion was tested by "the knife peel" method [12]. The results of the study indicate that epoxy coatings as a corrosion protection method will perform well in a pore solution environment if the coating is free of defects, damage and has good adhesion and thickness. Otherwise it will perform only slightly better than bare steel [12].

The surface conditions and careful handling of the material are two factors that are very difficult to control. Even with careful inspection it would be difficult to guarantee that epoxy coated steel was installed properly and was in good condition. The results of this study correlated the condition of the coating to its performance. Because the corrosion protection is sensitive to the thickness, the number of defects coupled with the amount of chlorides present in the environment, the performance of epoxy coating for any given project is difficult to predict.

An additional study on Virginia bridge decks by Pyc indicated that corrosion can begin prior to the arrival of chlorides at the coating-steel interface where debonding has occurred. Coating thickness and overall quality of the coating was found to be satisfactory but coating-steel bond problems are the "corner-stone" with respect to the long term performance of epoxy-coated reinforcement in concrete [13].

Study by the University of Wisconsin

Another study conducted at the University of Wisconsin by Pincheira (2008) assessed the corrosion protection performance of epoxy-coated reinforcing bars in four bridges located in Minneapolis-St Paul in Minnesota, over a period of 30 years [14]. This allowed the opportunity to study in an in-situ fashion the corrosion protection offered by epoxy coatings. The condition of the epoxy-coated steel was assessed by visual inspection, hardness testing, evaluation of the adhesion of the coating to the reinforcing steel, coating thickness measurement and bar corrosion estimation (Half-cell readings and Electrochemical Impedance Spectroscopy) [14]. The results from tests on epoxy-coated steel revealed that coating debonding with respect to the steel surface was found with and without rebar corrosion. Epoxy coated bars in all but one bridge had little to no corrosion damage.

Interim Report of the Virginia Transportation Research Council

An interim report of the Virginia Transportation Research Council has compiled a review on the performance of epoxy coated reinforcement from a number of studies across the United States and Canada. Some researchers found epoxy-coated reinforcing steel performing much better than the bare steel while others had reported just the opposite [15]. In areas such as the

Florida Keys and the Northeast Coast it has been observed that epoxy-coated reinforcing steel used in substructure elements and exposed to a marine environment is more susceptible to corrosion than the bare steel.

Bond characteristics of epoxy-coated strand to concrete are especially important in prestressed concrete members. After adhesion to the concrete is lost, the bond can only be developed by mechanical means such as friction. The frictional resistance depends on the surface conditions of the reinforcement material. Some surface roughness is necessary to promote frictional resistance [16]. This can be lost with a smooth epoxy coating. Free-end slip pull-out tests have been carried out on both black steel and epoxy-coated steel reinforcement and concluded that epoxy coatings significantly reduce the bond of the steel to concrete matrix [17].

2.3 Testing Bond Strength: North American Strand Producers, NASP Bond Test

In prestressing strand, the bond between the steel and the concrete matrix is provided by adhesion, mechanical interlock and friction. An applied load on the wire is resisted by interface shear stresses which depend on the interfacial bond characteristics between the wire and the surrounding concrete [18]. The initial stiffness achieved by the system is attributed to the adhesive component of bond. After adhesion has been overcome, mechanical interlock between the deformations and the surrounding concrete commences. This mechanical interlock continues until the concrete between the wire deformations has sheared off. After this, only the frictional component of bond remains [18].

The NASP Bond Test was developed as a standard test procedure to assess the bonding abilities of seven-wire prestressing strands with concrete [19]. The research extended for three rounds of investigations, each refining the procedure and setup. The current procedure is described in Round IV Report of the NASP test protocol, tested and written by Bruce W. Russell of the University of Oklahoma on behalf of the NASP Association. Researchers compared the results of the NASP Bond Test to the Moustafa and PTI tests and found the results of the former testing procedure to be more reproducible and repeatable [19].

The test consists of "pulling" a strand embedded in a confined mortar cylinder and measuring the force required to achieve 0.1in slip of the strand relative to the mortar. The details for the frame used in the NASP Round IV tests, is shown in Figure 2.1. It consists of a rigid frame were the test specimen is mounted. A 2in bond breaker is placed at the fixed end of the strand to prevent the presence of stress concentrations upon loading that can lead to cracking. A bond breaker can be any material that wraps around the strand and prevents the mortar from bonding to the steel at that section. The strand is then run through the steel mould after which the mortar is cast and consolidated in the steel cylinder that provides confinement.

The strand displacement is measured by a Linear Variable Differential Transformer (LVDT) mounted onto the steel casing. The mortar strength should be 4750 ± 250psi according to the revision made for Round IV without specifying any proportions of cement, water and aggregate. The pull-out test should be performed 24 ± 1hr after casting. Studies conducted in the NASP Round II concluded that the least variation in NASP values is exhibited when the pull-out value at 0.1 in. of end slip is used. Therefore, the current NASP Test requires the reporting of the pull-out force when the free end slip of 0.1 in. is achieved [19].

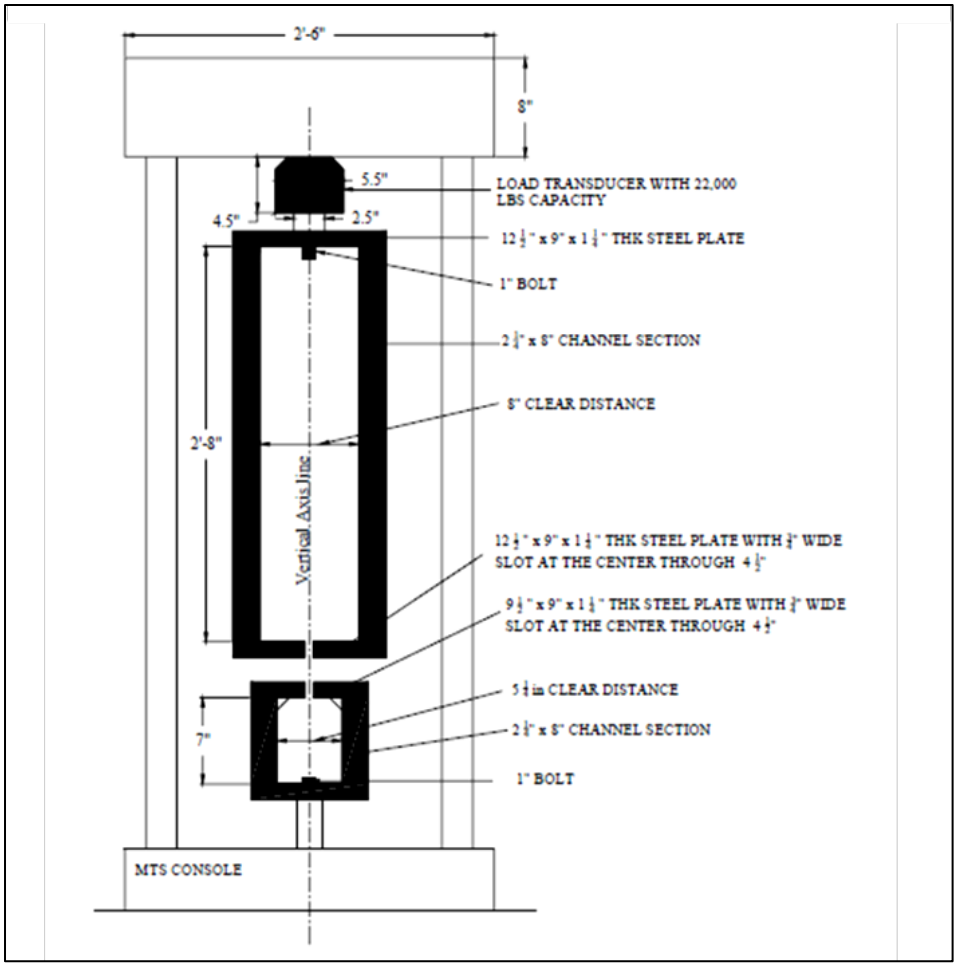

Figure-2. 1 NASP Bond Test Set-up as described in NASP Round IV

Chapter 3: Background on Corrosion

This chapter supplies a brief introduction to corrosion mechanisms in reinforcing carbon steel, and an overview of how to measure the resistance to corrosion in steel strands. Also, there are three different manufactures of steel strands studied in the present work, thus, one section of this chapter will describe the manufacturing process and discuss the major differences that can affect the coating process.

3.1 Corrosion Mechanisms in Reinforcing Carbon Steels in Concrete

Corrosion can be defined as the electrochemical reaction between a metal and its environment. For steel embedded in concrete, the general corrosion results in the oxidation of iron, Fe to Fe(III) with the formation of rust, Fe_2O_3. The volume of resulting iron oxides can be two to four times larger than the original Fe. Consequently, the pressure created on the surrounding concrete by this expansion leads to cracking and spalling of the concrete and subsequent loss of prestress transfer.

Reinforcing steel embedded in concrete shows a high amount of resistance to corrosion. The cement paste in the concrete provides an alkaline environment that protects the steel from corrosion. This corrosion resistance is due to the formation of a passive layer of iron oxides (a few nanometers thick and not well defined mineralogical composition) on the steel when exposed to the very basic conditions of the cement paste. This film is stable in the highly alkaline concrete (pH approx. 11-13). The general corrosion rate of steel in this state is negligible. The steel is unlikely to rust as long as the passivating conditions remain. However, under a critical concentration of certain chemical species in the concrete, CO_2 and

chlorides the passive layer suffers local breakdowns. It is known that the major mechanism by which steel embedded in concrete corrodes in presence of chloride is localized, or pitting corrosion [7].

Pitting corrosion is a form of localized corrosion of the metal surface that takes the form of small cavities or pits that can perforate the metal [20]. In addition, in the presence of an applied stress, pits can serve as sites to initiate stress-corrosion cracking [21].

Anodic reaction

Within the pit, which is regarded as a small hemisphere (see Figure 3.1) at the starting stage, the metal dissolution reaction is taking place as follows, where *M = metal*, *z = coefficient*, *e = electrons*.

$$M \rightarrow M^{z+} + ze^{-}$$

However, this is the only reaction within the pit that results in an electrical imbalance that attracts negatively charge ions, namely chloride ions. This reaction forms hydrochloric acid in the pit, once initiated and will continue:

$$M^{z+}Cl^{-}z + zH_2O \rightarrow M(OH)z + z(H^{+}, Cl^{-})$$

Pitting is considered to be autocatalytic in nature; once a pit starts to grow, the local conditions are altered such that further pit growth is promoted.

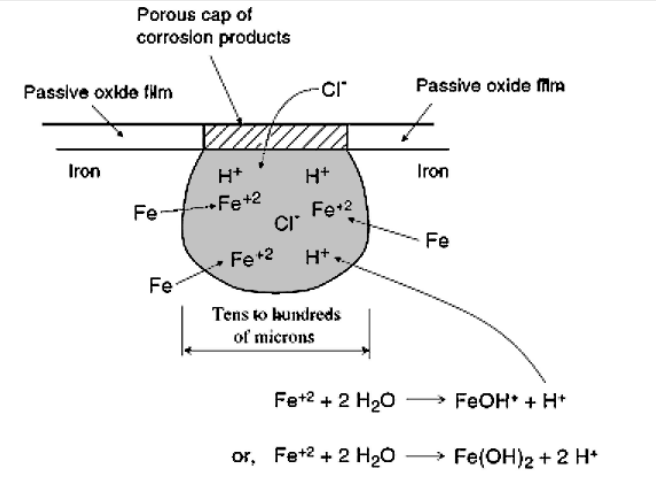

Figure-3. 1 Pitting Corrosion reactions and pit formation

Cathodic reaction

The growing pit can be regarded as an anodic region where electrons are produced. These electrons migrate to other regions of the surface still protected by the passive oxide film. Thus, the exposed surface outside of the pit will reduce oxygen to hydroxyl ion following the reaction:

$$O_2 + 2H_2O + 4e^- \rightarrow 4(OH^-)$$

As this process cathodically protects the region outside the pit, the metal dissolution region cannot spread laterally across the surface. In addition the large cathodic surface can maintain this reaction and form a large cathode to small anode ratio that will accelerate the anodic reaction and therefore increase the depth of the pit.

3.2 Electrochemical Methods for Corrosion Resistance Measurement

In order to evaluate different anticorrosion treatment one needs to assess the ability of the treated metals to withstand pitting corrosion in an adequate timeframe. Most laboratory corrosion tests are accelerated tests; the method of accelerating corrosion testing will depend upon the material being examined, the environment and the type of corrosion mechanism. Several common methods for acceleration of corrosion include increasing: aeration for immersion tests, temperature, pressure for stress corrosion cracking tests, acidity in immersion tests, relative humidity for atmospheric tests, concentration of the corroding electrolyte, anodic polarization of the electrode etc. For any accelerated test all the above mentioned variables should be carefully control to not alter the main corrosion mechanisms and the kinetics of several intermediate corrosion reactions leading to spurious results.

ASTM standards testing procedures have been set up for the various laboratory tests. Among these are Electrochemical Impedance and Potentiodynamic Anodic Polarization; Immersion (partial, total and intermittent); Salt Spray (Fog) Testing (Neutral, Acetic Acid, Cyclic Acidified, Cyclic Seawater etc).

The electrochemical tests have been used extensively in the study of passivity breakdown and the development of alloys resistant to pitting corrosion, specifically Potentiodynamic Anodic Polarization, had been used in order to obtain the value of pitting corrosion potential for the different treated metals. The tendency of a metal or alloy to undergo pitting is characterized by its critical pitting corrosion potential, E_{pit} [21].

The Potentiodynamic Anodic Polarization technique involves measuring current density versus the polarization potential while the potential is increase at more positive values at a constant rate. The output of this test will be a linear or semi-log plot of current, *I* (or current density, *i,)* versus potential, *E*. Once corrosion pits initiate, they usually propagate rapidly, represented by a sharp increase in current density at electrode potentials just beyond the critical pitting potential[21]. The *I* versus *E* graphs are known as polarization curves. *E* versus log *I* (or *i*) curves contain information on general corrosion potentials, general corrosion rates, passivation and pitting corrosion. While polarization curves provide quantitative information on general corrosion potential and information on passivation processes, the pitting potential is only a qualitative indicator of long-term corrosion in the field. For a given electrolyte, the pitting corrosion potential will not only depend on the surface finish of the metal but also will depend on the sweep rate. This rate should be very low, around 0.15 mV/s, so that it allows reaching a quasi steady state of the system at a given potential.

For a given chloride concentration and solution pH the more positive the critical pitting potential, the more resistant the metal or alloy is to pit initiation[21]. There is more than one way to read the pitting potential from a polarization curve. However, since this number is only good to compare different metals or anticorrosion treatments any way can be valid. One of the criterions for interpreting this parameter is shown in Figure 3.2. The critical pitting corrosion potential is taken as the potential value where a tangent to the polarization curve (in the positive current density region) intersects the x-axis, as shown.

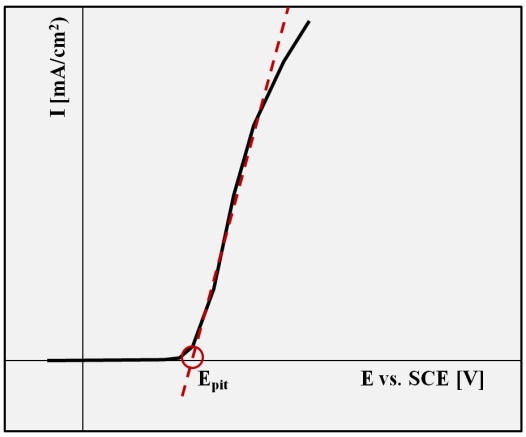

Figure-3. 2 Determination of Critical Pitting Corrosion Potential using polarization plots

3.3 Material Properties: Steel Strand Manufacture

The strand manufacturing process generally includes the following steps: (1) cleaning and pre-treating 0.5in steel rods in an acid solution and water, (2) drawing the wire through a series of 8 dies using several lubricants, (3) winding the six outer wires around the king wire to form the 7-wire strand, (4) the strand is drawn in tension through an induction furnace, (5) lastly the strand is rinsed in re-circulating water and then packaged [22].

The surface condition of the steel is primarily affected by the pretreatment and lubricants used in the drawing of the wire. For the coating process, it is the lubricants used in production of the strand that can negatively affect the coating-steel bond. The two most common lubricants used in the industry are calcium and sodium stearate. These are composed of calcium or sodium hydroxides and stearic acid. Calcium stearate is preferably used due to its more effective coating quality and the lower cost as compared to sodium

stearate [22]. Calcium stearate is particularly troublesome as it is insoluble in water and therefore extremely difficult to remove.

The specific manufacturing process of Sumiden strand was provided by this manufacturer: The wire rod was pickled in sulfuric acid to remove scale and rinsed in water twice, followed by dipping in a borax pre-coating process. The wire rod was then cold drawn through 9 dies using a calcium base lubricant on all dies. The seven spools of wire were then placed in the stranding machine and formed into the strand. Next, the strand was placed under tension using two capstans and induction heated to a minimum temperature of 380°C. The strand was then cooled in the cooling troughs.

Chapter 4: Coating Quality

4.1 Introduction

The objective of the studies presented in this chapter is to determine the optimal combination of pre-coating surface conditioning and coating thickness that renders more noble (positive) pitting corrosion potentials. The nature of the substrate surface is a determinant factor on the quality of coatings, independently of their nature and way of deposition [23]. The performance of a coating is significantly influenced by its ability to adhere properly to the substrate material. The presence of even small amounts of surface contaminants, oil, grease, oxides etc. can physically impair and reduce coating adhesion to the substrate. Selection of the proper method for surface preparation depends mainly on the substrate and the coating selected.

In the particular case of dip coating a surface using an aqueous sol the wettability of the substrate surface is also key player in the successful deposition of uniform film. Materials with high surface energy wet very well by water solutions and are known as hydrophilic; they have the ability to form hydrogen bonds between surface and water molecules [24].

Steel surfaces are expected to be hydrophilic, especially in the case of carbon steel since when exposed to air they develop a chromic or ferric oxide film. However, our experience indicates otherwise. In order to obtain uniform coatings with metal oxide sols these surfaces must be further oxidized by firing the metal in air at 300 ^{o}C [25]. Hyun-Su Kim et al. [24] reported a large increase in the hydrophilicity of the SS304 when treated in the He-O_2 and Ar-O_2 plasmas. The authors explain this increase of wettability by the enrichment of the

surface in iron and chromium oxides, such as Fe_2O_3, FeOOH, Cr_2O_3, and CrO_3, which contain hydrophilic functional groups.

The thickness of the oxide film using dip coating is a function of the oxide concentration in the sol, the withdrawn speed and the number of dip coatings performed. It would seem intuitive that the thicker the oxide film the more effective it will be as a barrier to protect the surface. However, in the literature of inorganic nanoporous coatings it is well accepted that thicker films are more prompt to detach from the substrate and crack during the drying and firing process. The critical thickness to avoid cracking depends on the morphology and size of the oxide nanoparticles, the strength of adhesion to the substrate and its roughness.

Anodic Polarization and SEM are the testing methods used in this chapter. To evaluate the effectiveness of the various combinations the critical pitting potential for each combination is measured and compared to a controlled experiment in which a steel wire with no surface treatment or coating is subjected to the anodic sweep.

In this study a sol of zirconia, ZrO_2, TiO_2 or a combination of the two was used in the preparation of the coatings. All strands, labeled in this work as Steel-A, were from the same manufacturing company, Sumiden Wire Products. This is a 0.6in Grade 270 low-relaxation strand with individual wires measured at 5 ± 0.10mm (0.197 ± 0.004in) in diameter.

4.2 Materials and sample preparation

This section details the preparation of the inorganic coatings that will be used on the steel wires for all testing in this research.

4.2.1 Coating Preparation

The sols are made from three ingredients: water, nitric acid (HNO_3) and either Titanium IV Isopropoxide ($Ti(OPr^n)_4$) or Zirconium IV Propoxide ($Zr(OPr^n)_4$). For the Zirconia sol, 1000mL of high purity water were mixed with 20mL of nitric acid in a 2000mL flask and stirred constantly by a magnetic stirrer [26]. While stirring constantly, 73.33mL of $Zr(OPr^n)_4$ was added to the acidic solution which quickly precipitates. The precipitates are stirred constantly for three days until peptized. The pH of the sol was measured as 0.88, a value too acidic to promote the formation of ZrO_2 particles. A quick check of the chemical equilibrium diagram for the system revealed that the pH of the solution must be close to a value of 2 to obtain enough large particles of ZrO_2 before starting the dialysis process. Otherwise, many of the ZrO_2 would be lost in the dialysis process.

Over the next two days small increments on the order of 5mL of sodium hydroxide (NaOH) were added to the sol to increase the pH of the solution. A total of 99.7mL of 2.5M NaOH were added to the solution to obtain a final pH of 1.84 before dialysis. 200ML of the sol was dialyzed for 3 hours in 5 liters of acidic H_2O with a pH of 2.7. After 3 hours, the acidic water was replaced by another of the same pH and the sol was allowed to dialyze for one day. Following the 24 hours, the change in dialyzing water was repeated and the sol was dialyzed for one additional day. The final pH of the zirconia sol at this point was 2.95.

The procedure for the titania sol is similar to that of zirconia with some differences: 556.64ml of water, 398mL of HNO_3 and 45.37mL of $Ti(OPr^n)_4$ were mixed in the same manner as for the zirconia sol. The resulting pH of the solution was acceptable and the sol was processed through the dialysis membranes without the need to titrate the solution. The final pH of the Titania sol was of 3.00 after dialysis. Figure 4.1 shows a photograph of the dialyzed sols. Because the metal oxide particles of ZrO_2 are so small the sol appears clear.

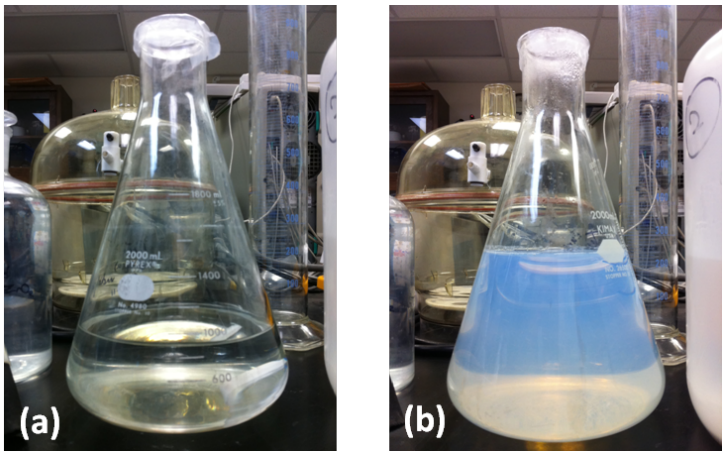

Figure-4. 1 (a) zirconia (ZrO_2) sol, (b) titania (TiO_2) sol

4.2.2 Coating Application

Dip-coating was chosen as the most economical and practical technique to apply the coatings onto the steel wires. The procedure is simple and involves the dipping of the wire into the solution, withdrawing at a constant rate and then sintering the coating on the wire.

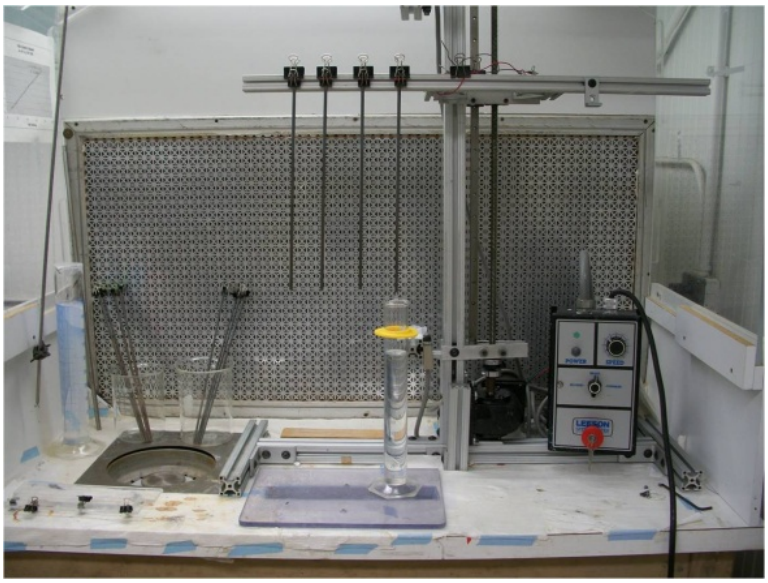

Figure-4. 2 Dip coater used for coating application

First the steel wire was dipped using the dip-coater shown in Figure 4.2 and allowed to dwell in the solution for 30 seconds. The wire was then removed at a constant speed of 3mm/s and allowed to dry in air for a few minutes. After each dip the wire is then heated to 80°C for 10min to completely dry and seal the layer of coating. After depositing 4 layers, the wire was then sintered by heating from room temperature to 350°C at a rate of 10°C/min and allowed to dwell at 350°C for 1 hour before being cooled to a finishing room temperature of 30°C at a rate of 10°C/min. After this heat-treatment, if more layers were to be added, the process was repeated, always finishing in a heat treatment to obtain the resulting ceramic coating on the substrate.

4.3 Test Setup and Instrumentation

A typical set-up for an anodic polarization experiment consists of a two or three-electrode cell. The former cell consists of the working electrode (the sample) and a counter electrode. In a three-electrode cell the third electrode (a reference) is included to reduce the effect of additional polarizations in the cell [27]. A three-electrode cell was used for this study. In this case the potential of the working electrode is measured with respect to the reference electrode. The counter electrode in this cell completes the circuit and transmits current to or from the working electrode. Figure 4.3 shows the electrochemical cell used for the experiment, the electrode arrangement and electrolyte container.

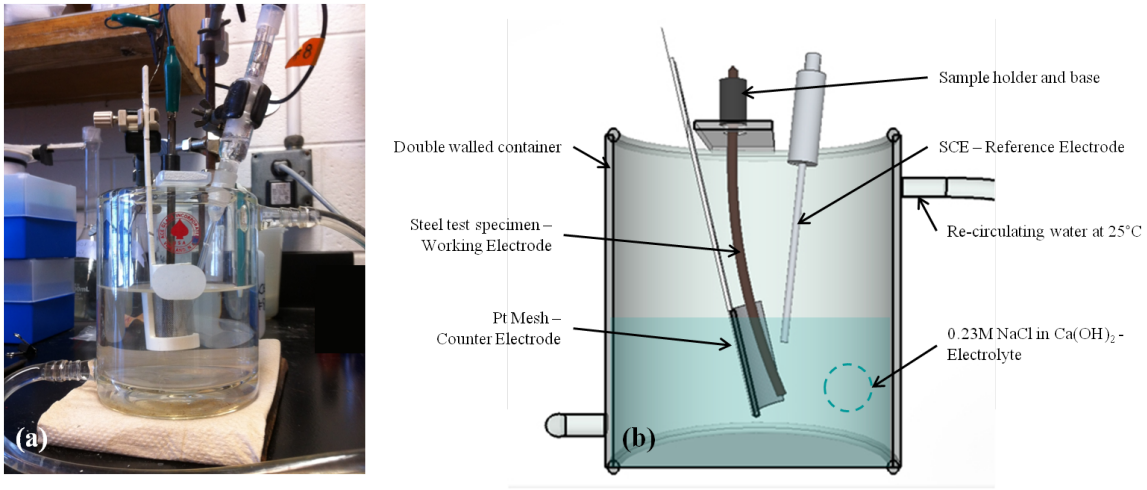

Figure-4. 3 Three-Electrode Cell used for the polarization Experiments

The working electrode was a 4.5in long steel wire extracted from the strand. The wire was clamped to a holder which was then placed on a plastic base. The exposed end of the wire was then covered with enamel to prevent corrosion from selectively starting at the edges. A

platinum mesh, attached to a PVC frame for stability, was used as a counter electrode. Lastly, a saturated calomel electrode (SCE) was used as the reference electrode. The electrodes were connected to the multichannel potentiostat which applies the voltage sweep and measures the current produced in the cell.

To simulate the environment found in concrete the steel wires were submerged in a 12.4 pH electrolyte consisting of a 0.23M NaCl in $Ca(OH)_2$ saturated solution. Temperature was maintained constant for all experiments in this work. A re-circulating water bath was used to keep the temperature of the electrochemical cell at a constant 25°C.

The parameters for the technique are entered into the program shown in Figure 4.4 and all data is recorded in the computer. The program for this anodic polarization experiment starts with a 30min rest period in which the system is allowed to achieve equilibrium at the open-circuit potential. After this time, the potential is swept across the desired range. This range varied for several of the experiments, due to heterogeneity of the steel surface. For some samples the critical pitting potential would only start to be discernible near the range limit which would decrease the amount of data necessary for proper analysis. Varying this value does not affect the results only the data range. The voltage is swept from the most negative value to the most positive at a rate of 9.96 mV/min (0.166mV/s) until reaching a limiting voltage value or a user defined max current value, in this case 140mA.

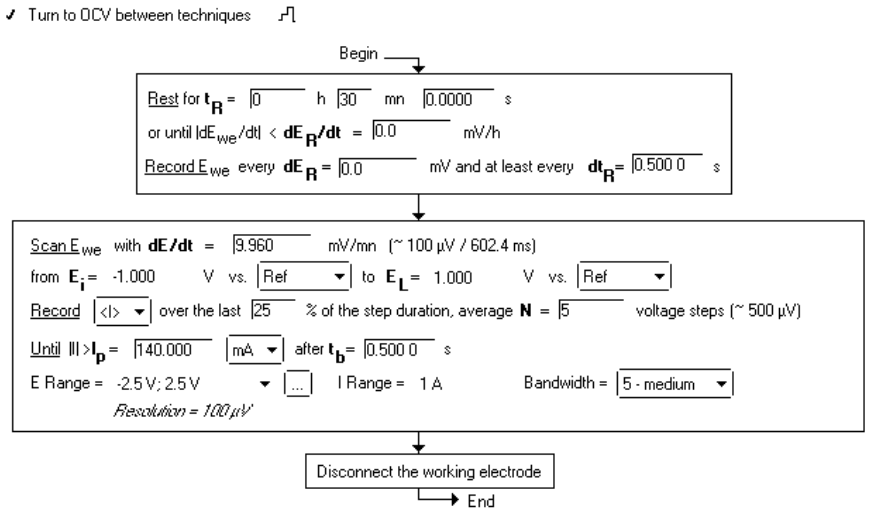

Figure-4. 4 Potentiodynamic Anodic Polarization Program

4.4 Results

Output from the Anodic Polarization technique is retrieved as current versus potential plots. The plots shown in this section have been normalized for any differences in surface area of the wires and plotted as current density (*i*) versus potential (*E*). The potential values refer to the potential of the working electrode versus the reference electrode potential (SCE).

The following sections detail the effect of coating thickness before and after applying a surface treatment. The effect of various surface treatments was also studied. Finally zirconia and titania coatings were compared.

4.4.1 Effect of coating thickness

A. No pre-coating surface treatment

Steel wires with no surface treatment and no coating (bare) were subjected to the anodic polarization voltage sweep and the resulting voltage recorded. Using the method described in Section 1.1.4 the average critical pitting corrosion potential for these specimens was recorded as 143mV. Coated wires showed a small increase in the critical pitting corrosion value of 7 and 33 percent for 8 and 12 layers of ZrO_2 respectively. Table 4.1 and Figure 4.5 show the critical pitting potential values and anodic polarization curves.

Table-4. 1 Critical Pitting Corrosion Potentials for bare and coated wires with no surface treatment prior to coating application

Sumiden-Sample ID	E_{pit} [mV]	Avg. E_{pit} [mV]	% Increase
A-steel270-uncoated-washed-01	-120	-143	NA
A-steel270-uncoated-washed-02	-130		
A-steel270-uncoated-washed-03	-180		
A-steel270-ZrO2-washed-4L-01	40	-133	7.0 %
A-steel270-ZrO2-washed-4L-02	-200		
A-steel270-ZrO2-washed-4L-03	-240		
A-steel270-ZrO2-washed-8L-01	-50	-97	32.6 %
A-steel270-ZrO2-washed-8L-02	-100		
A-steel270-ZrO2-washed-8L-03	-140		

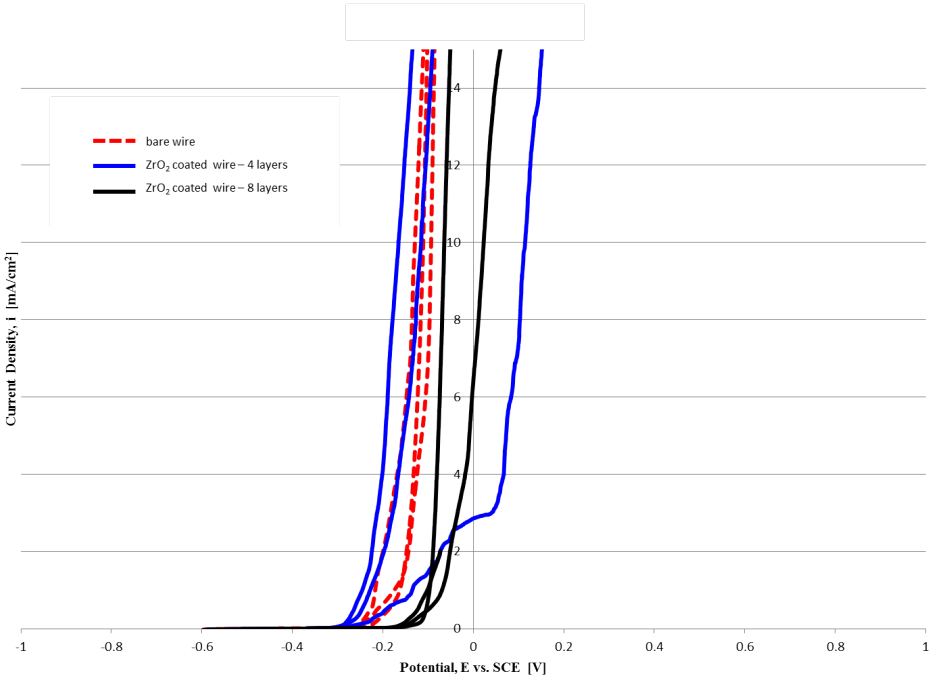

Figure-4. 5 Polarization Curves: bare wire (red), coated with 4 layers of ZrO_2 (blue), coated with 8 layers of ZrO_2 (black) with no surface treatment.

It should be noted that while the coating should have a smooth dark finish on the steel surface the coated samples in this section were opaque and dusty as shown in Figure 4.6 It was surmised that the coating had gelled. This having been the case, the coating had to have been exposed to a basic solution. The hypothesized solution was a calcium compound possibly found in lubricants used during strand production as discussed in Section 1.1.5.

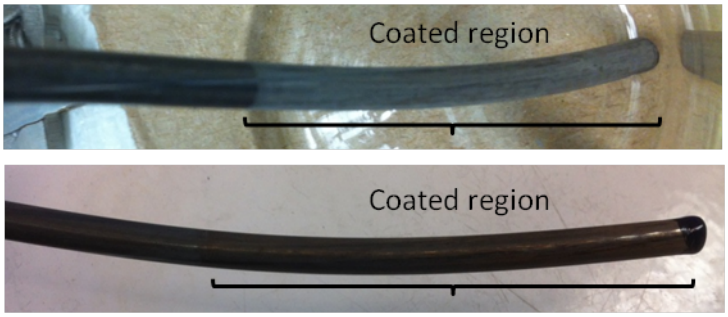

Figure-4. 6 (top) gelled coating on steel wire, (bottom) clear coating on steel wire

To counter the basic environment of the steel surface hydrogen peroxide (H_2O_2), hydrochloric acid (HCl) and Nitric acid (HNO_3) were used as surface conditioning treatments prior to coating the steel.

B. With pre-coating surface treatments

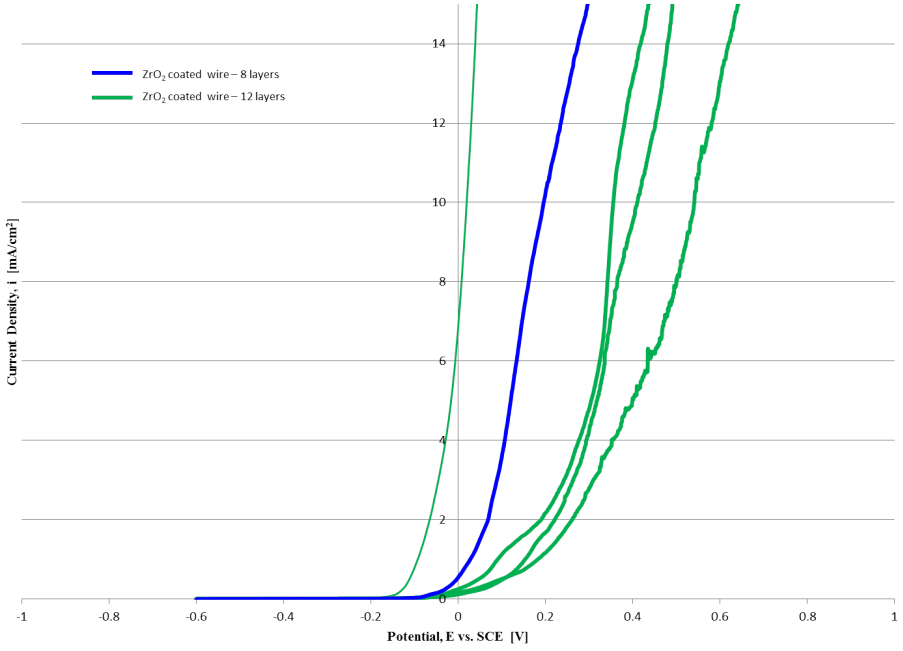

Figure-4. 7 Polarization Curves for H_2O_2 pre-treated wires, coated with 8 layers (blue) and 12 layers (greens) of zirconia.

The anodic polarization curves in Figure 4.7 correspond to steel wires treated with H_2O_2. The *blue* curve corresponds to 8 layers of coating while the *green* curves correspond to 12 layers of coating. One can note by a simple inspection of the curves that the point at which the current increases exponentially has moved to a more positive potential, indicating a higher resistance to pitting. This is a good indication of the performance of the coating as corrosion

protection. From these two set of samples it can be observed that thicker coatings offer better corrosion protection and that surface conditioning prior to coating is necessary to improve the effectiveness of the coating.

4.4.2 Effect of pre-coating steel-surface treatment

A. H_2O_2 vs. HCl

The hydrogen peroxide pretreatment consisted of first heating for 20min a basic solution of H_2O_2 in NaOH with a pH equal to 13. Next the wires are introduced into the solution and heated to the same 70°C for 30min. The wires are then removed from the solution, washed in soap and tap water and rinsed in high purity water followed by ethanol.

The hydrochloric acid pretreatment consisted in immersing the steel wires for 30min in a HCl solution with pH equal to 4. The wires were then removed from the acid, washed in soap and tap water and then rinsed in high purity water followed by ethanol.

Two wires treated with HCl and two wires treated with H_2O_2 prior to coating were studied by anodic polarization. Simple inspection of the curves tells one that a slightly better result can be achieved with a H_2O_2 pretreatment. Critical pitting corrosion potetial for these curves and others in this section are included in Section-A of the Appedix Chapter.

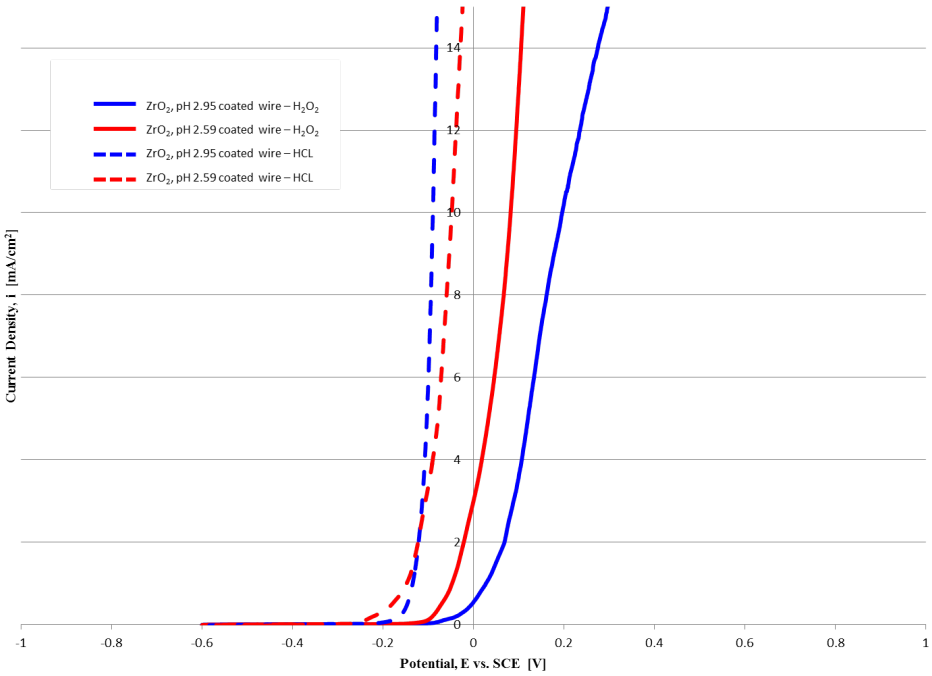

Figure-4. 8 Polarization Curves for H_2O_2 and HCl pre-treated wires coated with 8 layers of zirconia coating of 2.59 and 2.95 pH

The plot on Figure 4.8 also includes a comparison of two zirconia coatings with different coating pH. The result was inconclusive and was decided to continue with the more acidic coating of higher concentration.

B. H_2O_2 vs. HNO_3

The increase in critical pitting potential relative to wires coated with no prior surface treatment other than just rinsed in water is shown in Table 4.2. The clear winner here is the H_2O_2 surface treatment, followed by the nitric and hydrochloric acids. The polarization plots for these results are shown in Section-A of the Appendix chapter.

Table-4. 2 Critical Pitting Corrosion Potential Increase for H_2O_2 and HNO_3 pre-treatments

Sumiden-Sample ID	Pretreatment	E_{pit} [mV]	Avg. E_{pit} [mV]	% Increase
A-steel270-ZrO2-washed-8L-01	None	-50	-97	NA
A-steel270-ZrO2-washed-8L-02		-100		
A-steel270-ZrO2-washed-8L-03		-140		
A-steel270-ZrO2-pH2.95-H2O2-8L-01	H_2O_2	40	30	131.0 %
A-steel270-ZrO2-pH2.59-H2O2-8L-01		20		
A-steel270-ZrO2-pH2.95-HCl-8L-01	HCl	-110	-105	-8.6 %
A-steel270-ZrO2-pH2.59-HCl-8L-01		-100		
A-steel270-ZrO2-HNO3+350C-8L-01	HNO_3	-140	-140	-44.8 %
A-steel270-ZrO2-H2O2+HNO3-8L-01	HNO_3 + H_2O_2	40	-15	84.5 %
A-steel270-ZrO2-H2O2+HNO3-8L-02		-70		

4.4.3 Titania (TiO_2) vs. Zirconia (ZrO_2) Coatings

Table 4.3 summarizes the critical pitting corrosion potential values for three wires coated with titania and a combination of both titania and zirconia coatings. The percent increase is expressed with respect to wires surface treated with H_2O_2 and coated with 8 layers of zirconia. Sample 1T was coated with 2 layers of titania followed by 4 layers of zirconia. The particle concentration of titania is almost double that of zirconia and thus the number of layers is reduced by half to have a comparable coating thickness. This coating resulted in a decrease of pitting potential. Samples *2T* and *3T* were coated with 4 layers of titania. The steel surface of *2T* was immersed for 30min in H_2O_2 while *3T* was immersed for 1hr. It was important to see if any changes in time of pretreatments could improve the adhesion of the coating to the steel substrate.

Table-4. 3 Critical Pitting Corrosion Potential Increase for titania coated wires

	Sumiden-Sample ID	E_{pit} [mV]	Avg. E_{pit} [mV]	% Increase
1T	A-steel270-TiO2+ZrO2-H2O2-1hr-01	0	0	-100.0 %
2T	A-steel270-TiO2-H2O2-1hr-01	0	0	-100.0 %
3T	A-steel270-TiO2-H2O2-30min-01	-240	-240	-900.0 %

4.4.5 Discussion

After testing various combinations of pre-coating steel-surface treatments, steel surface conditions, coating types and thickness and sintering temperatures the optimum combination was tested on strand from all manufacturers in order to study new variables and conditions. From the results of Chapter 3, a surface treatment of H_2O_2 in which the wire is immersed in the solution for 30min at a temperature of 70°C yielded a more effective coating adhesion. Little or no gelling of the coating was observed with this pretreatment. In addition, the zirconia coating proved more effective and increasing the number of layers or coating thickness improves pitting corrosion resistance. A number of 8 layers of zirconia coating were used for the tests described in subsequent chapters. The sintering temperature was maintained at 350°C and the surface roughness was not altered. Finally, wires removed from the strand were used for all testing in this chapter.

The presence of calcium compounds on the steel surface was then corroborated by Scanning Electron Microscopy (SEM) and Energy Dispersive Spectroscopy (EDS). The results from these analyses are presented in the following section.

4.5 Microstructure of Uncoated Wire Surfaces

The presence of calcium was detected in small quantities by the *X-ray Line Scan* Energy Dispersive Spectroscopy (EDS) technique in which a beam follows a path drawn on the image and produces a plot of elemental atomic percentages along the length of the vector line. The atomic percentage of iron (Fe), carbon (C), calcium (Ca) and oxygen (O) are plotted in Figure-4.9. The graphs represent quantity of elements found in a 0.4mm vector line. From the graph and vector line it can be seen that light areas correspond to higher atomic percentages of iron while darker areas contain around 65% oxygen, which indicates the presence of oxides. Some presence of calcium (23 atomic %) can be observed along the vector line in Figure-4.10. The Fe and O counts indicate the presence of pure iron and magnetite (Fe_3O_4).

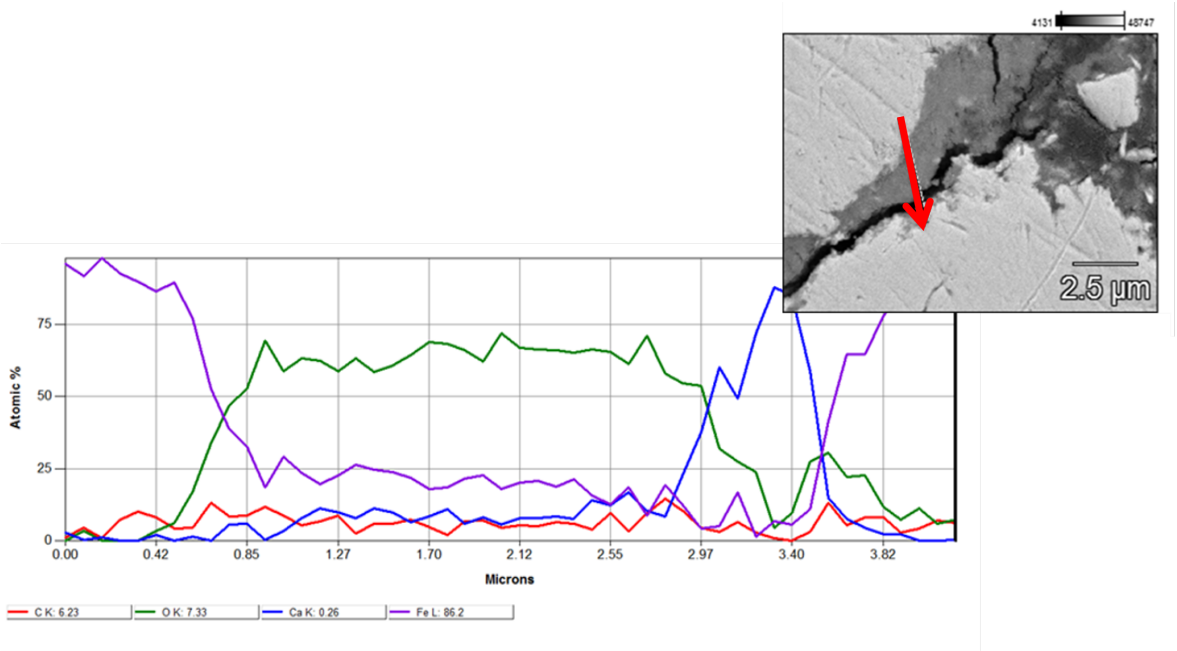

Figure-4. 9 EDS Spectra in atomic % of line scan vector shown in photo (top). The x-axis corresponds to the length of the line vector. Light areas are indicative of iron while gray areas are generally oxides.

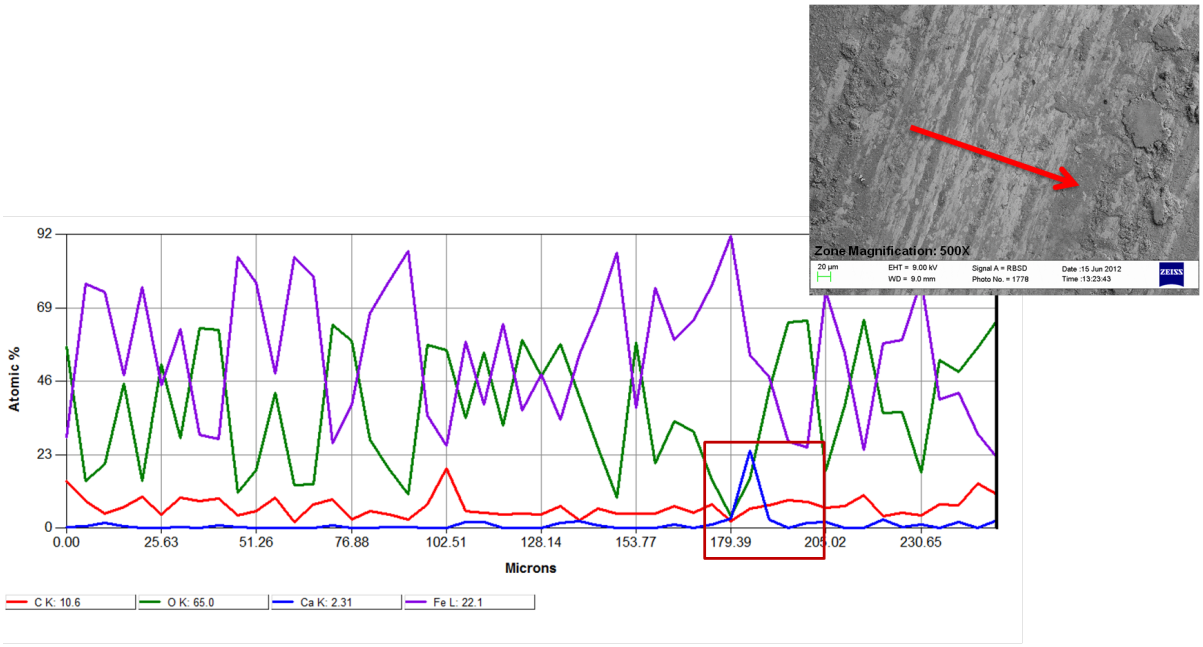

Figure-4. 10 EDS Spectra in atomic % of line scan vector shown in photo (top). The x-axis corresponds to the length of the line vector. Blue peak indicates presence of calcium

Chapter 5: Corrosion Protection

5.1 Introduction

This chapter relates to the effects that an applied tensile stress will have on the microstructure of the coating and its ability to protect against pitting corrosion. High tension is applied to pre-stressing steel strand when casting a prestressed concrete member. The strand is then cut and a resulting compression force is transferred to the concrete, giving prestressed members their high strength. It is therefore necessary to evaluate how the coating will perform under these conditions.

Each steel strand producer follows a slightly different manufacturing process for their product that results in slightly different surface finishes. In this chapter we also study the influence that the surface finish will have on the coating application and performance. For this purpose, strands from three manufacturers were tested. Differences in pitting corrosion potentials between un-stretched and stretched coated wires and between each manufacturer were studied electrochemically by the same anodic polarization test discussed in Chapter 4.

5.2 Materials and sample preparation

The coating used for the tests discussed in this chapter is solely zirconia, ZrO_2, prepared by the method described in Chapter 4. The wires were extracted by cutting the strand in 4.5in segments with an abrasive saw. Both straight and curved wires from all three manufacturers were used for this test. In addition all wires, both the bare and coated, were pre-treated with

the surface treatment described in Chapter 4. The steel was immersed in a pH 13 solution of 30% (or 9.79M) H_2O_2 in 3M NaOH for 30min and then rinsed in tap water, high purity water and finally ethanol.

To test the ability of the coating to resist the tensile stresses to which the strand will be subjected to in a real world application, a tension force equal to 80% of the steel's ultimate tensile strength was applied to bare and coated wires. These specimens are labeled *Stretched* in Table 5.2. After reaching 80% of the ultimate load, the wires were quickly released. A 10,000lb capacity MTS console with round grips was used to apply the tensile load at a rate of 0.1in/min. The tension load was applied after the wires were coated with 8 layers of ZrO_2.

The labeling used for each manufacturer and the measured diameter of wires is shown in Table 5.1. All wires are Grade 270 low-relaxation steel obtained from 7 wire prestressing strand. Wires were also tested in the stretched and un-stretched condition with and without the coatings. The number of samples for each manufacturer and variable is shown in Table 5.2.

Table-5. 1 Strand labeling and diameter

Manufacturer	Designation	Wire Diameter
Sumiden Wire Products	Steel-A	5±0.10mm
Insteel Wire	Steel-B	5±0.10mm
American Spring Wire	Steel-C	4.1±0.10mm

Table-5. 2 Wire condition and coating for polarization experiment

Number of Specimens for each variable combination						
	Steel-A		Steel-B		Steel-C	
Wire Condition	Bare	Coated	Bare	Coated	Bare	Coated
Not Stretched	3	3	3	3	3	3
Stretched	3	3	3	3	3	3

5.3 Test Setup and Instrumentation

The setup for this test follows the same procedures as discussed in Chapter 3. A 3-electrode cell is used to measure the current-potential relationship to obtain the critical pitting corrosion potential. Single 4.5in steel wires were used for this experiment. Coated wires were covered with 8 layers of the zirconia coating after receiving a H_2O_2 treatment. Bare wires were also pre-treated with H2O2 to homogenize the surface.

5.4 Results

The critical pitting corrosion potentials values are reported in this section. The *E* values refer to the potential of the working electrode versus the reference electrode potential. The polarization plots for each manufacturer are plotted in Section-B of the Appendix.

5.3.1 Effect of coating on pitting corrosion resistance of steel wire (not subjected to tension stress) for all manufacturers in the study.

The average pitting potential of bare and coated wires is plotted in Figure 5.1 for manufactures Steel-A, Steel-B and Steel-C. Coated wires show more positive pitting corrosion potentials than bare wires for all manufactures. The increase in pitting potential varies from one manufacturer to the other and this is largely due to the surface conditions achieved by the manufacturing process of each producer.

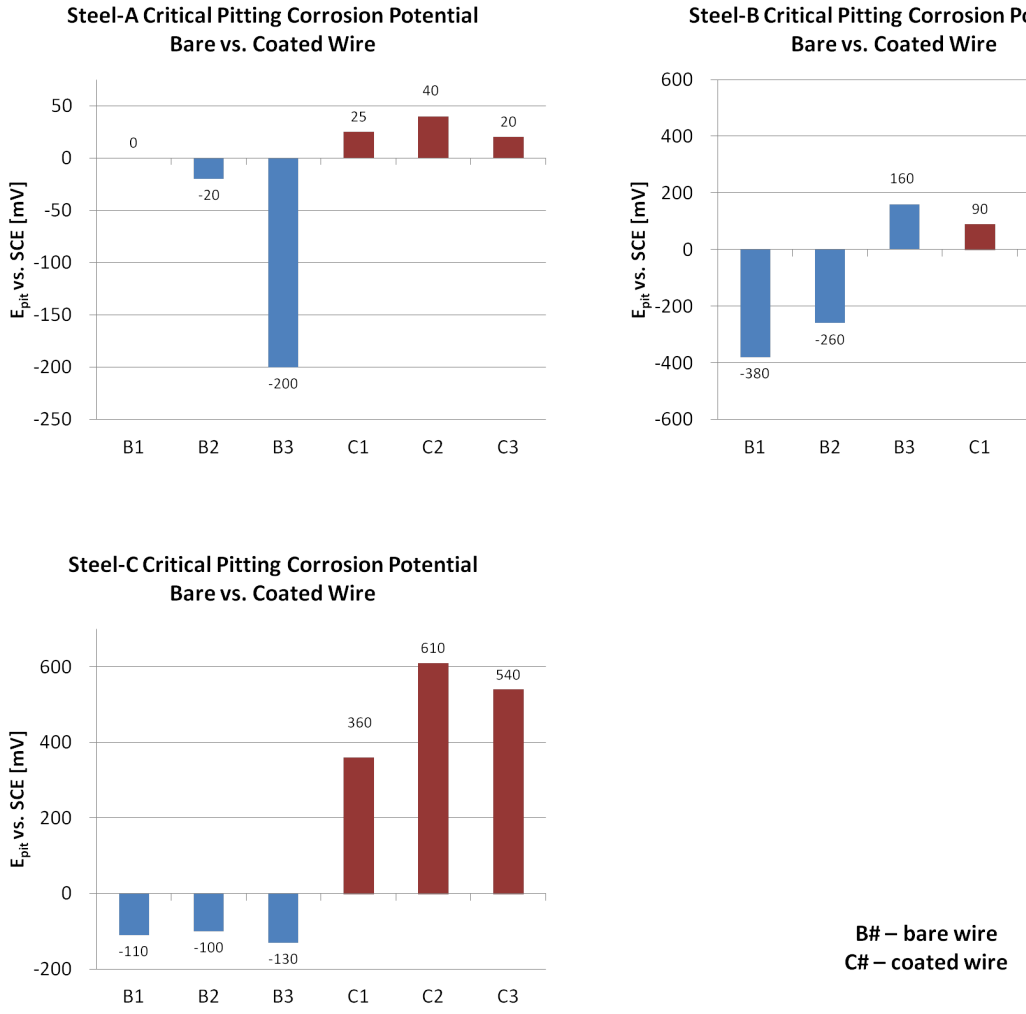

Figure-5. 1 Critical Pitting Potentials of un-stretched wires

Table 5.3 summarizes the amount of average critical pitting corrosion potential increase of coated wires for each manufacturer with respect to bare wire.

Table-5. 3 Change in pitting corrosion potential and level of corrosion protection for each strand manufacturer

Manufacturer	Δ Epit [mV]	Level of Corrosion Protection
Steel - A	396.67	Fair
Steel - B	101.67	Poor
Steel - C	616.67	Good

The surfaces of the wires were examined by SEM in order to investigate the differences in quality and microstructure of the coatings for all manufacturers in the study. Figures 5.2, 5.3 and 5.4 show the surface of coated wires from manufacturers A, B and C respectively with cracks in the coating denoted by arrows. Steel-C has a rougher surface (more grooves) compared to Steel-A and B. However, Steel-A and B have sites with large defects while other sites show none. Lack of coating homogeneity results in "weak spots" where pitting nucleation is promoted.

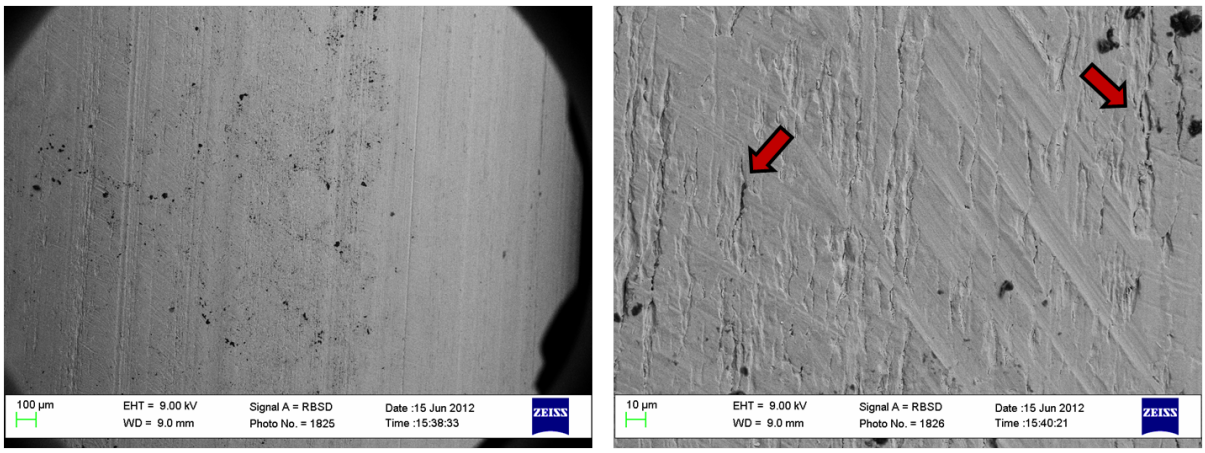

Figure-5. 2 Steel-A Surface microstructure of steel wire coated with 8 layers of zirconia. Cracks in the coating are denoted by arrows.

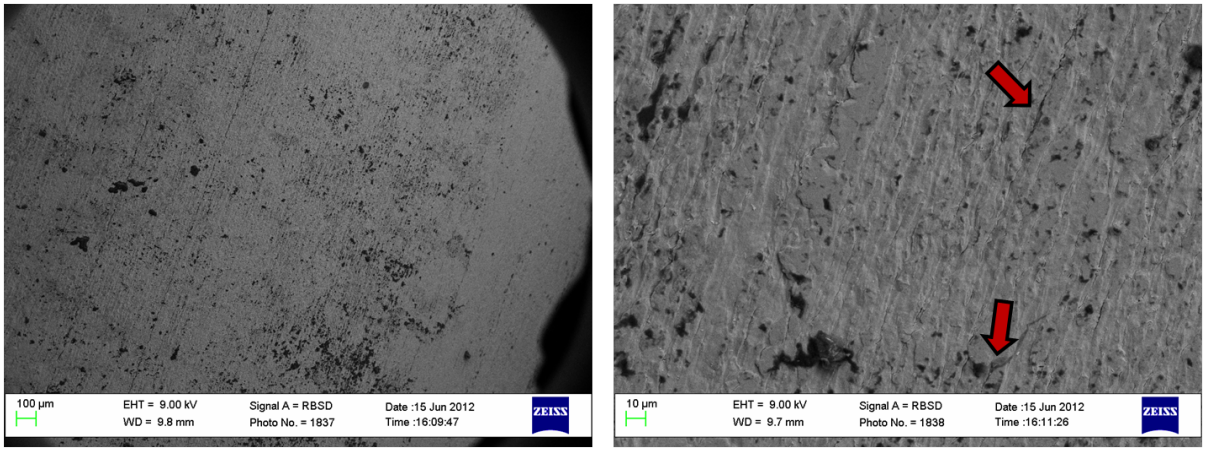

Figure-5. 3 Steel-B Surface microstructure of steel wire coated with 8 layers of zirconia. Cracks in the coating are denoted by arrows.

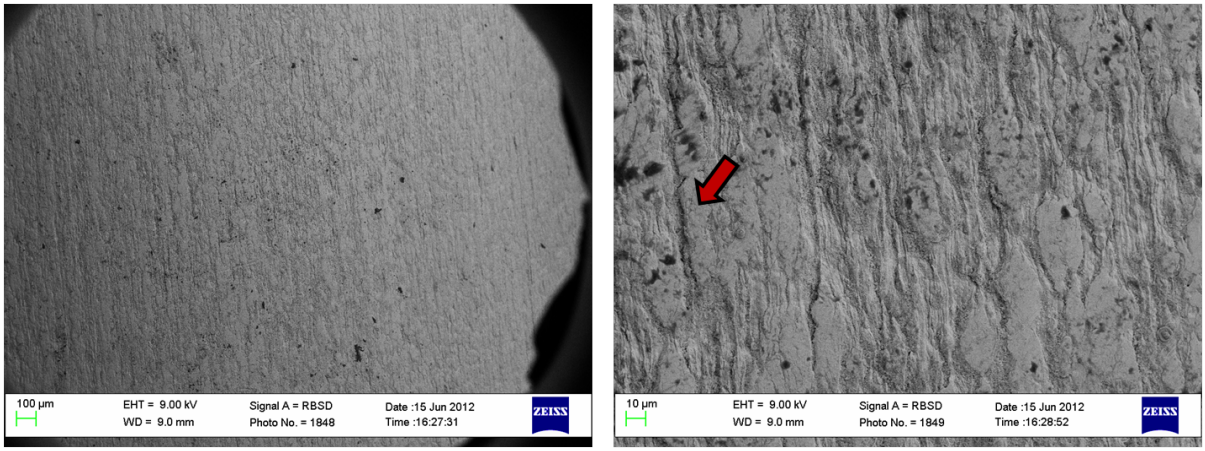

Figure-5. 4 Steel-C Surface microstructure of steel wire coated with 8 layers of zirconia. Cracks in the coating are denoted by arrows.

5.3.2 Effect of coating on pitting corrosion resistance of steel wire (subjected to tension stress)

The average pitting potential of bare and coated wires is plotted in Figure 5.5 for manufacturers A, B and C. In this case there is no increase in critical pitting potential values of coated samples with respect to bare wire. Coated wires performed poorly for all steels. The difference of averaged pitting corrosion potential values is tabulated in Table 5.4.

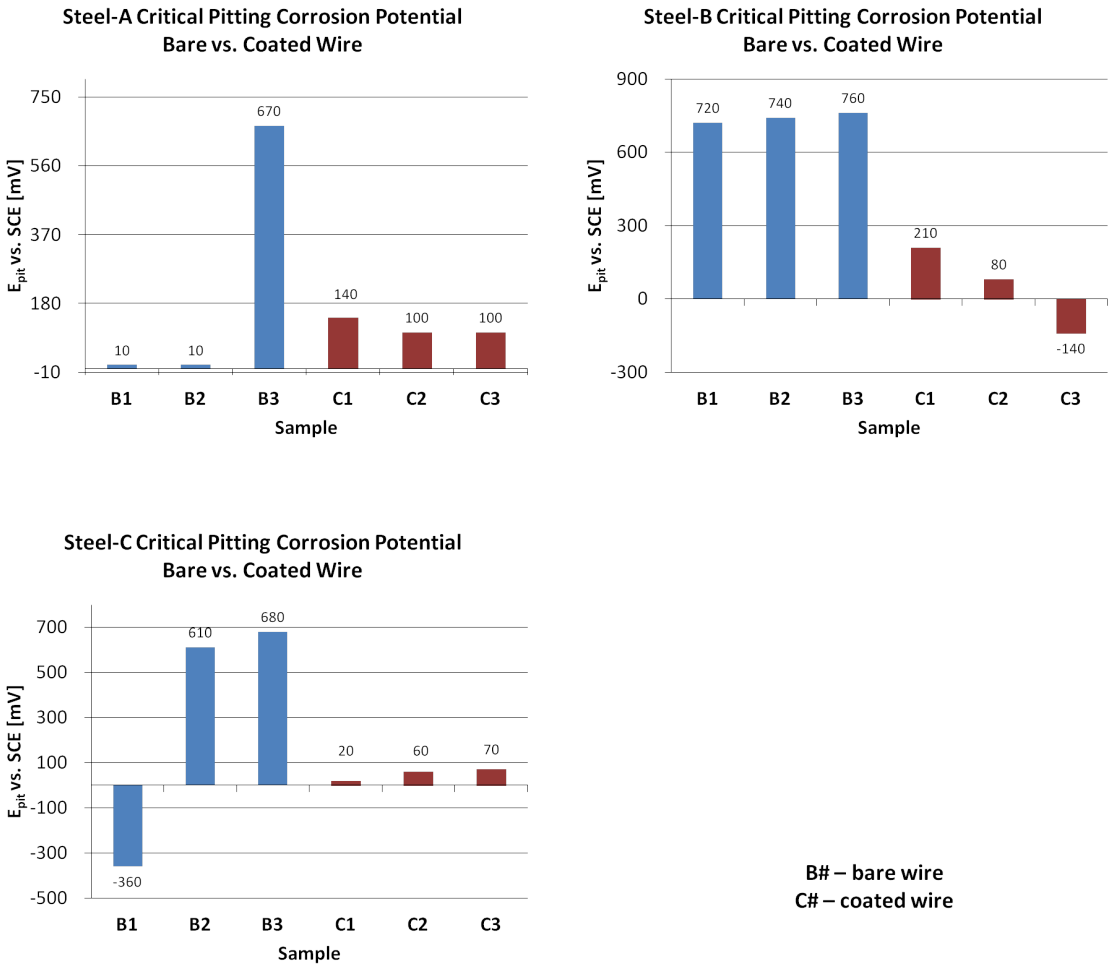

Figure-5. 5 Critical Pitting Potentials of stretched wires

Table-5. 4 Change in pitting corrosion potential and level of corrosion protection for each strand manufacturer.

Manufacturer	Δ Epit [mV]	Level of Corrosion Protection
Steel - A	-690.00	None
Steel - B	-116.67	None
Steel - C	-260.00	None

SEM micrographs were obtained for the surfaces of coated wire and coated wires subjected to tension. The surface was studied for signs of any cracks on the coating. When we compared un-stretched and stretched wire from Steel-A in Figure 5.6 more cracking was observed in the latter. For Steel-B and C, as illustrated in Figures 5.7 and 5.8 respectively, no significant increase in cracks was observed. On the other hand, some increase in surface roughness can be observed in Figure 5.7 for Steel-B.

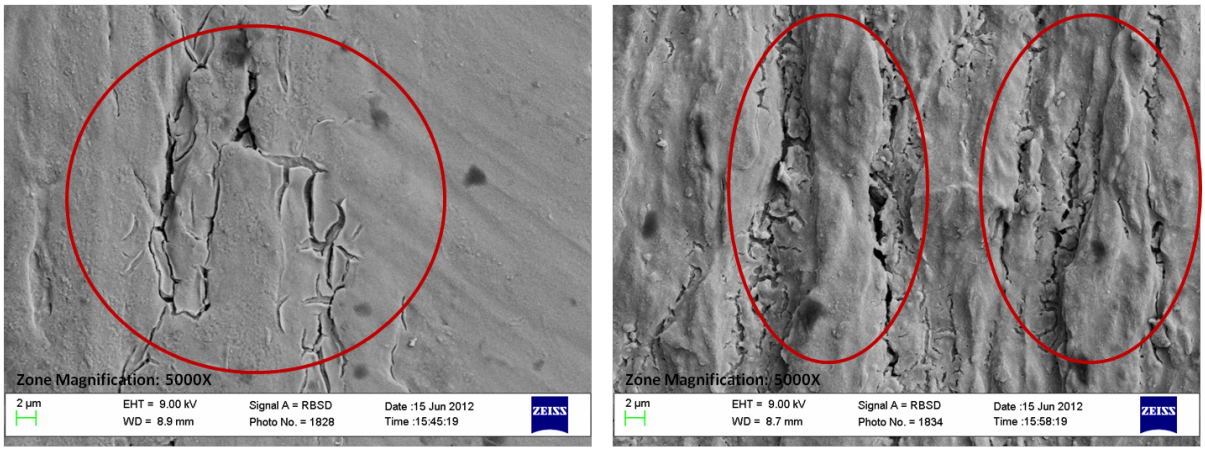

(a) coated/un-stretched

(b) coated/stretched

Figure-5. 6 Steel-A Surface microstructure of steel wire coated with 8 layers of zirconia and subsequently stretched. Cracks in the coating are circled.

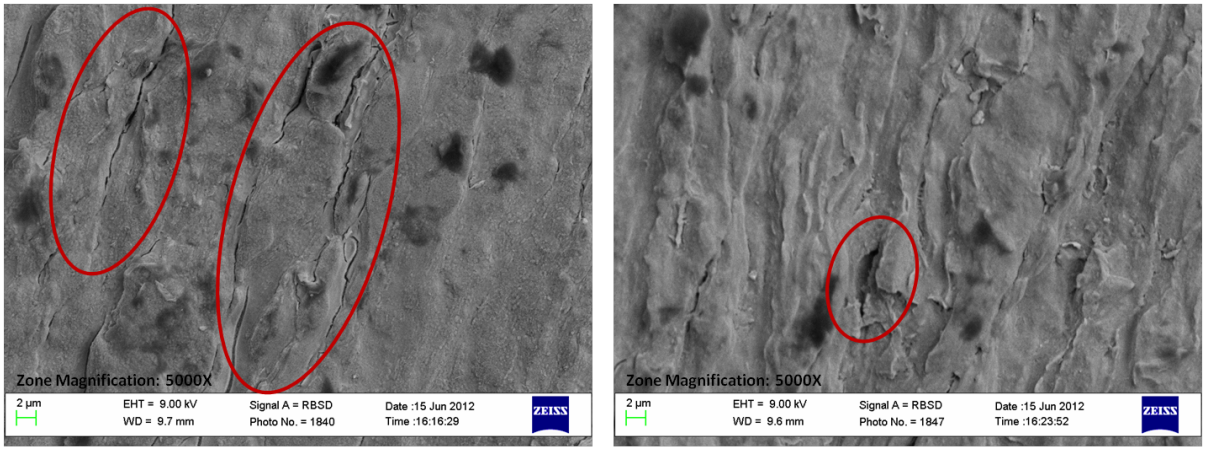

(a) coated/un-stretched (b) coated/stretched

Figure-5. 7 Steel-B Surface microstructure of steel wire coated with 8 layers of zirconia and subsequently stretched. Cracks in the coating are circled.

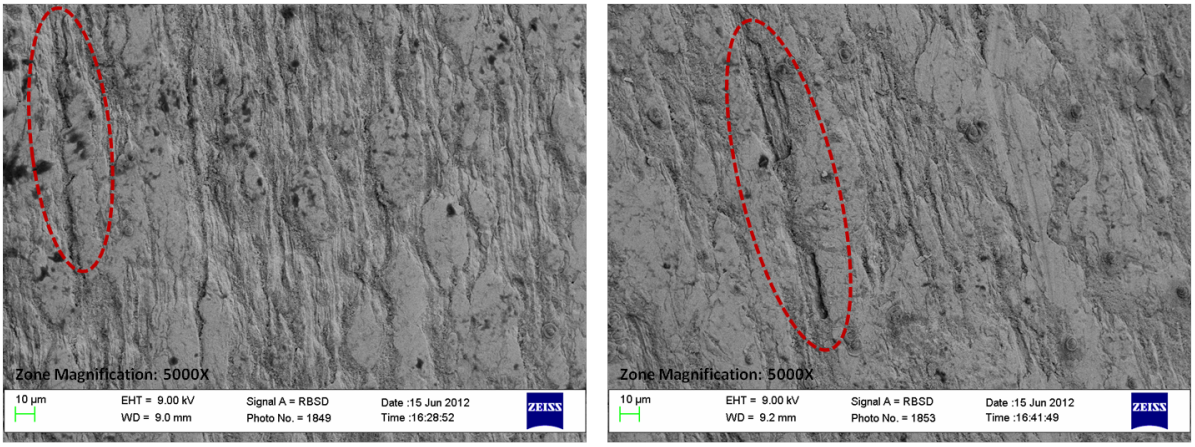

(a) coated/un-stretched (b) coated/stretched

Figure-5. 8 Steel-C Surface microstructure of steel wire coated with 8 layers of zirconia and subsequently stretched. Cracks in the coating are circled.

Note on data deviation:

The anodic polarization technique is sensitive to variations in the electrode surface. The steel strand does not present the same exact surface conditions, at the micro level, throughout its length. Therefore each wire, obtained from the strand, will have a varying number of "weak spots" which will affect somewhat the incubation of pits on the steel surface.

Table 5.5 summarizes the critical pitting potential values for each sample, the average value and the deviation of each test corresponding to one of 4 variables: bare, coated, un-stretched and stretched wire.

Table-5. 5 Average critical pitting corrosion potential values for all samples

Test Specimen ID – Steel-A	**E_{pit} [mV]**	**[mV]**	
A-Steel270-H2O2-uncoated-01	-380	**Average**	**Std. Dev.**
A-Steel270-H2O2-uncoated-02	-260	-160.0	283.5
A-Steel270-H2O2-uncoated-03	160		
A-Steel270-H2O2-ZrO2-01	90	**Average**	**Std. Dev.**
A-Steel270-H2O2-ZrO2-02	120	236.7	228.5
A-Steel270-H2O2-ZrO2-03	500		
A-Steel270-H2O2-uncoated-stretch-01	720	**Average**	**Std. Dev.**
A-Steel270-H2O2-uncoated-stretch-02	740	740.0	20.0
A-Steel270-H2O2-uncoated-stretch-03	760		
A-Steel270-H2O2-ZrO2-stretch-01	210	**Average**	**Std. Dev.**
A-Steel270-H2O2-ZrO2-stretch-02	80	50.0	176.9
A-Steel270-H2O2-ZrO2-stretch-03	-140		
Test Specimen ID – Steel-B	**E_{pit} [mV]**	**[mV]**	
B-Steel270-H2O2-uncoated-01	0	**Average**	**Std. Dev.**
B-Steel270-H2O2-uncoated-02	-20	-73.3	110.2
B-Steel270-H2O2-uncoated-03	-200		
B-Steel270-H2O2-ZrO2-01	25	**Average**	**Std. Dev.**
B-Steel270-H2O2-ZrO2-02	40	28.3	10.4
B-Steel270-H2O2-ZrO2-03	20		

B-Steel270-H2O2-uncoated-stretch-01	10	**Average**	**Std. Dev.**
B-Steel270-H2O2-uncoated-stretch-02	10	230.0	381.1
B-Steel270-H2O2-uncoated-stretch-03	670		
B-Steel270-H2O2-ZrO2-stretch-01	140	**Average**	**Std. Dev.**
B-Steel270-H2O2-ZrO2-stretch-02	100	113.3	23.1
B-Steel270-H2O2-ZrO2-stretch-03	100		
Test Specimen ID – Steel-C	**E_{pit} [mV]**	**[mV]**	
C-Steel270-H2O2-uncoated-01	-110	**Average**	**Std. Dev.**
C-Steel270-H2O2-uncoated-02	-100	-113.3	15.3
C-Steel270-H2O2-uncoated-03	-130		
C-Steel270-H2O2-ZrO2-01	360	**Average**	**Std. Dev.**
C-Steel270-H2O2-ZrO2-02	610	503.3	129.0
C-Steel270-H2O2-ZrO2-03	540		
C-Steel270-H2O2-uncoated-stretch-01	-360	**Average**	**Std. Dev.**
C-Steel270-H2O2-uncoated-stretch-02	610	310.0	581.3
C-Steel270-H2O2-uncoated-stretch-03	680		
C-Steel270-H2O2-ZrO2-stretch-01	20	**Average**	**Std. Dev.**
C-Steel270-H2O2-ZrO2-stretch-02	60	50.0	26.5
C-Steel270-H2O2-ZrO2-stretch-03	70		

5.4 SEM Analysis of stretched steel surface

SEM micrographs of coated and stretched wires show an increase in surface roughness upon stretching and subsequent relaxation. However, it seems that the zirconia coating goes along with this change in topography reasonably well, although with some increase in cracking. Still this does not explain the large decrease in corrosion protection upon stretching of the wires.

It will be interesting to learn what happens in the interlayer between the zirconia and the steel surface. The decrease in corrosion protection may be due to the coating being no longer bonded to the steel. For this purpose we examined the cross-sections of these wires by SEM.

Unfortunately, at present, we only have data on cross sections for uncoated wires. However, we believe that the findings are interesting in themselves to be reported. Micrographs of un-stretched and stretched bare steel wire cross-section are shown in Figure 5.9.

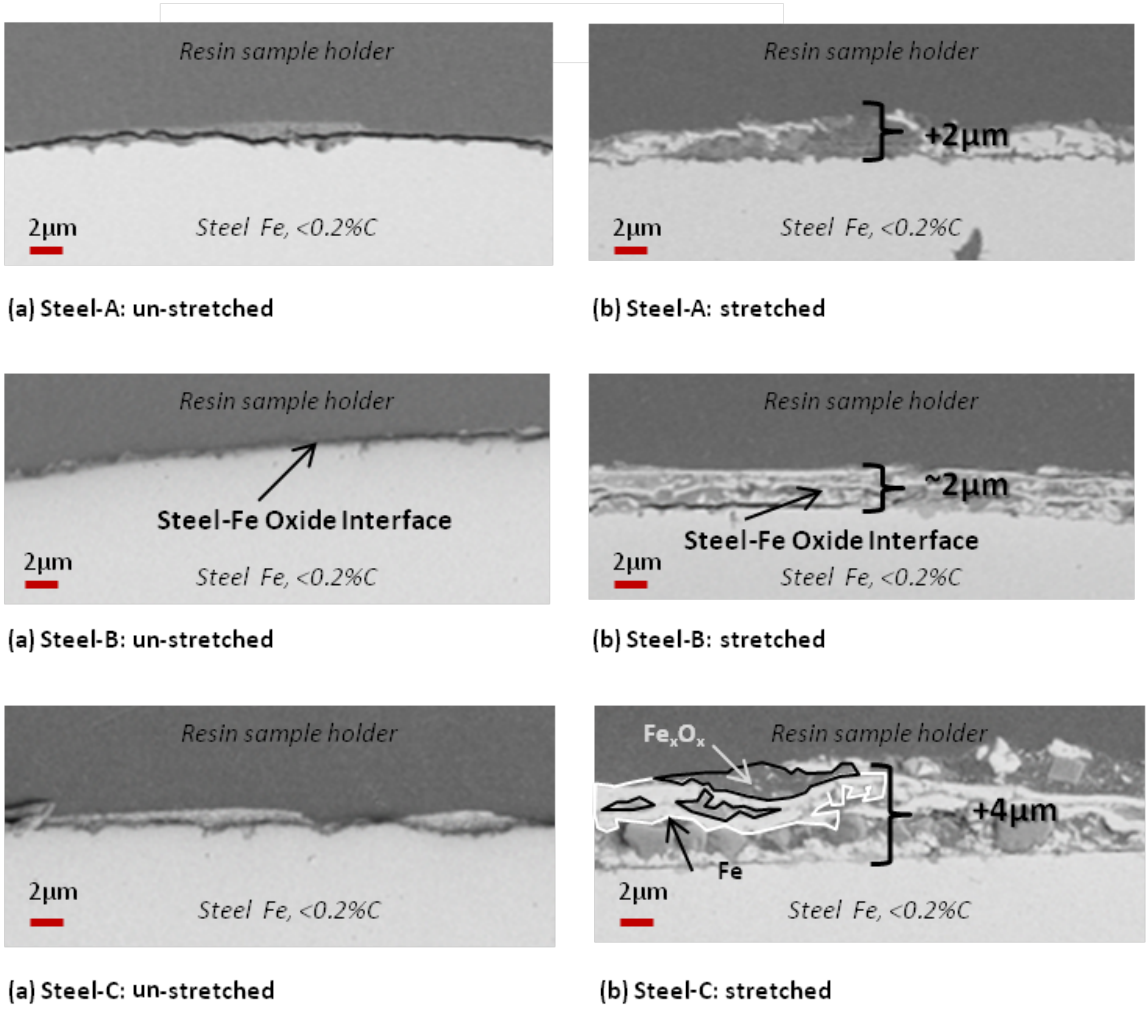

Figure-5. 9 SEM photographs of the iron – iron oxide interface before and after stretching the wire. The dark smooth area above the interface corresponds to the epoxy resin sample holder and the white area below corresponds to pure iron. Iron oxides can be seen as gray areas within the interface.

From these cross-section micrographs a tendency emerges. The interface between the iron oxide surface layer (that include Fe_3O_4 and Fe_2O) and the iron core has more than quadrupled in thickness after subjecting the wire to tension. Another important observation is that several layers of iron, identified in Figure 5.9 have "peeled off" from core and moved into the interface. This change in the steel surface can affect the adhesion of the coating, promote cracks and induce oxidation of the iron that has migrated to the interface.

Chapter 6: Bond Strength Evaluation: Small-Scale NASP Pull-Out Test

6.1 Introduction

While the coatings should be effective as a corrosion protection method they should also not be detrimental to the structural behavior of the prestressed member. In prestressing applications high strength and crack control is achieved by applying an internal tension-compression couple through prestress transfer. Sufficient bond between the steel and concrete must be developed so that the design prestress is successfully transferred to the concrete. To determine whether the metallic inorganic coatings will affect in any way the steel-concrete bond strength pull-out tests were performed by following the procedures described in this chapter.

The test described in this chapter is based on the NASP Bond Test described in the NCHRP 603 Report. It consists of "pulling" the steel strand from a concrete mortar cylinder and measuring the force required to achieve sufficient slip of the strand relative to the mortar. The concrete mortar was mixed in conformance with ASTM C192. The cement used was

Type III, same as used in precast applications. The sand conformed to ASTM C33 and the strand was tested by the manufacturers and should conform to ASTM 416.

6.2 Materials and Sample Preparation

Grade 270 low-relaxation 7-wire prestressing steel strand was used for this project. Three manufacturers provided the strand: Sumiden Wire Products, Insteel and American Spring Wire. The corresponding diameters and labeling used for this study is tabulated below:

Table-6. 1 Wire designation and properties

Manufacturer	Designation	Low Relaxation	Grade	Strand Diameter	Wire Diameter
Sumiden Wire Products	Steel-A	Yes	270	0.6in	5±0.10mm
Insteel Wire Products	Steel-B	Yes	270	0.6in	5±0.10mm
American Spring Wire	Steel-C	Yes	270	0.5in	4±0.10mm

The 7-wire strand for each manufacturer was cut into 13.5in long segments and the center wire was extracted to be coated with the nanoporous zirconia coating. Coated wires were pretreated with the basic H_2O_2 solution discussed in Chapter 3 and dip-coated in the zirconia sol to 10in of its length. Bare wires were only rinsed in tap water and ethanol in order to test the condition in which they are found in the field. Table 6.2 summarizes the sample size and variables. One batch of mortar was mixed for two bond tests that used strand from the same manufacturer.

Table-6. 2 Number of samples and variables

	Manufacturer					
	Steel-A		**Steel-B**		**Steel-C**	
	Mortar Batch 1		Mortar Batch 2		Mortar Batch 3	
Strand Condition	Bare	Coated	Bare	Coated	Bare	Coated
No. Cylinders	*4*	*4*	*4*	*4*	*4*	*4*

The target one-day strength for this test was 4500psi. The sand-cement ratio was 1.70 and the water-cement ratio was 0.37. The plastic molds for the cylinders where drilled at the base to accommodate the wire and were sealed with a plastic cap which had also been drilled to run the wire through the mortar. Before placing the mortar in the cylinder mould, a 1in long piece of tape was wrapped around the wire to act as a bond breaker. The wire was then inserted into the cylinder. The cylinders were filled halfway with mortar and vibrated using a vibrating table. Next, the moulds were filled completely and vibrated to eliminate air voids. A plastic cap was drilled in the center, for the wire to pass through, and placed over the cylinders to seal the mortar. The cylinders were then moist cured for 24 hours.

6.3 Test Setup and Instrumentation

The setup described in the NASP Bond Test specifications and the small-scale tests differ in four aspects: (1) test specimen, (2) size of the concrete mortar cylinder, (3) casting of the mortar and (4) the testing frame.

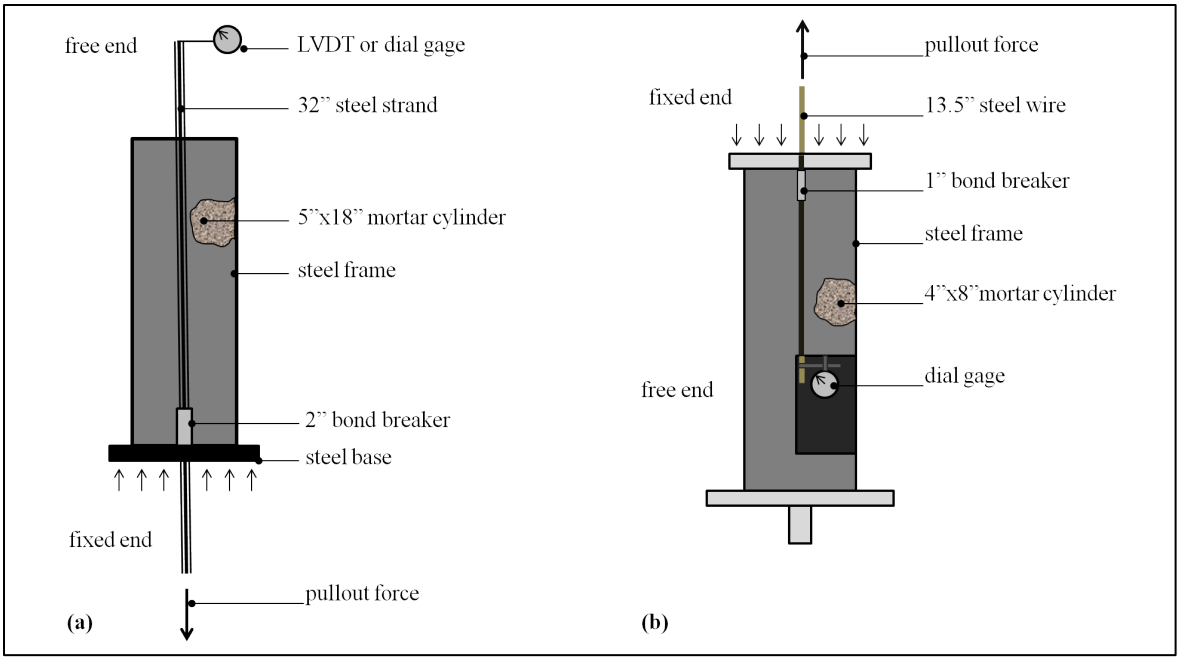

Figure-6. 1 (a) NASP Bond Test setup and (b) Small-Scale Bond Test setup

A comparison of the two test setups is shown in Figure 6.1. The NASP Bond Test requires the test specimen to be a 32in long 7-wire strand with an embedment length of 16in. The small-scale counterpart used a single 13.5in long center wire obtained from the 7-wire strand. The embedment length was 8in with a de-bonded section of 1in.

Secondly, because of the change in test specimen, the size of the cylinder was modified from a 8in by 15in cylinder to a smaller 4in by 8in cylinder. It should also be noted that in the NASP test the mortar is cast into the steel mould, while in this test, the mortar was cast into 4in by 8in plastic cylinders. Once cured, the cylinders were broken from the mold and placed inside the steel frame for testing. Lastly, the testing frame was altered and manufactured specifically for this test. The frame consists of a hollow steel cylinder with a metal perforated cap and a removable base. The confinement offered by this assembly is limited. However,

high confinement is not necessary in this case. A steel casing is required to prevent the concrete from cracking and spalling during testing, as this would not occur in the field. For this small-scale version, a single, straight, smooth wire was used that did not cause sufficient stress to induce cracking during testing.

A 10,000lb capacity MTS SINTECH tension/compression console shown in Figure 6.2 was used for this test. A rubber-bearing pad was placed on the mortar cylinder on the fixed end to prevent cracking. The mortar cylinder with the embedded wire was inserted into the steel frame through the bottom opening. The wire was secured to the top grip on the moving crosshead and the base was attached. The base is then anchored to the bottom, fixed grip. At this point the dial gage is attached to the strand with a holder so that the plunger is in contact with the bottom of the mortar cylinder. The rate of displacement was set at 0.1in/min. The pulling force was applied until the slip reached a value of 0.1in after which the test was terminated by the user.

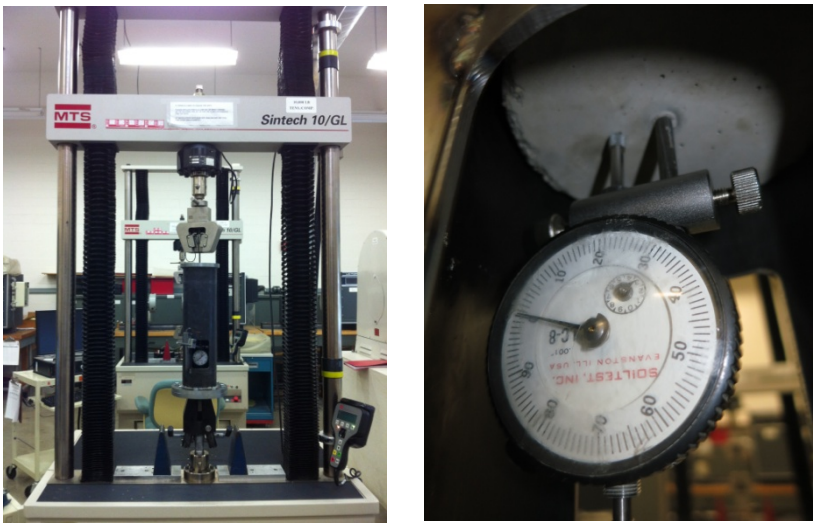

Figure-6. 2 (left) MTS console used for testing and (right) dial gauge attachment

6.4 Results

From the bond test four parameters were recorded: pull-out force at 0.10in of slip, maximum pull-out force, mortar strength and mortar flow. Table 6.3-4 summarizes the bond test results for bare and coated Steel-A wire. Coated wires showed an increased in pull-out force of 63% with respect to bare wire. The max pull-out load had a 140% increase.

Table-6. 3 Bond Test results for Steel-A bare wire

Test	Pull-out force at 0.1in (lbf)	Max Load (lbf)
A-none-01	206.9	699.3
A-none-02	111.7	410.4
A-none-03	216.8	619.1
A-none-04	64.8	320.1
Average	**150.0**	**512.2**
Std. Dev.	*74.0*	*176.7*
f'c	4579 psi	
Mortar Flow	163	

Table-6. 4 Bond Test results for Steel-A coated wire

Test	Pull-out force at 0.1in (lbf)	Max Load (lbf)
A-ZrO2-01	116.3	903.6
A-ZrO2-02	166.7	1068.6
A-ZrO2-03	402.2	1617.3
A-ZrO2-04	294.2	1318.1
Average	**244.9**	**1226.9**
Std. Dev.	*128.9*	*311.1*
f'c	4579 psi	
Mortar Flow	163	

For Steel-B however, pull-out force decreased by 56%, whereas the maximum pull-out load had an 83% increase. Pull-out values are show in Table 6.5-6.

Table-6. 5 Bond Test results for Steel-B bare wire

Test	Pull-out force at 0.1in (lbf)	Max Load (lbf)
B-none-01	410.0	434.9
B-none-02	463.1	478.7
B-none-03	574.5	574.5
B-none-04	326.3	409.3
Average	**443.4**	**474.4**
Std. Dev.	*103.9*	*72.6*
f'c	5155 psi	
Flow	136	

Table-6. 6 Bond Test results for Steel-B coated wire

Test	Pull-out force at 0.1in (lbf)	Max Load (lbf)
B-ZrO2-01	199.0	800.0
B-ZrO2-02	137.2	810.2
B-ZrO2-03	214.4	788.9
B-ZrO2-04	237.3	1074.1
Average	**197.0**	**868.3**
Std. Dev.	*42.8*	*137.5*
f'c	5155 psi	
Flow	136	

The third manufacturer showed a decrease in pull-out force and an increase in maximum pull-out load of 31% and 79% respectively.

Table-6. 7 Bond Test results for Steel-C bare wire

Test	Pull-out force at 0.1in (lbf)	Max Load (lbf)
C-none-01	206.5	407.3
C-none-02	259.9	489.3
C-none-03	302.4	439.6
C-none-04	NA	
Average	**256.3**	**445.4**
Std. Dev.	*48.0*	*41.3*
f'c	5059 psi	
Flow	163	

Table-6. 8 Bond Test results for Steel-C coated wire

Test	Pull-out force at 0.1in (lbf)	Max Load (lbf)
C-ZrO2-01	200.7	816.5
C-ZrO2-02	257.5	959.6
C-ZrO2-03	89.1	895.1
C-ZrO2-04	165.2	524.6
Average	**178.1**	**798.9**
Std. Dev.	*70.5*	*192.0*
f'c	5059 psi	
Flow	163	

All mortar batches were consistent in terms of strength and flow. The pull-out force for coated wires did not increase for all manufacturers, increasing for Steel-A and decreasing for Steel-B and C. The maximum pull-out force however increased for all manufacturers for coated wires by a factor of 2. The load plots and bar graph comparisons can be found Section-C of the Appendix to this report.

Chapter 7: Tension Tests on Individual Wires

7.1 Introduction

As part of the coating process, the wire and coating must be sintered at 350°C for 1-hour. This process could act as a form of annealing to the steel and negatively affect its mechanical properties and required strength. In order to test this possibility, tension tests were performed on center "king" wires in "as-received" condition and heat-treated to the sintering temperature of 350°C to obtain three important parameters: (1) modulus of elasticity, (2) ultimate tensile strength and (3) breaking strength.

7.2 Materials and Sample Preparation

The wires were not coated for this test as this procedure only evaluates the effect of heating with respect to the mechanical properties of the wire. The strand was cut into 8in long segments and only the center wire was used for testing in order to reduce the effect of wire curvature, induced by the stranding process.

The modulus of elasticity for reinforcing steel shall be taken as 29,000ksi. However, prestressing steel, the modulus of elasticity, E, is provided by the manufacturer. The modulus of elasticity is taken as the slope of the stress-strain (σ_o-ε) curve obtained from the tension test using the original cross-sectional area, where the extensometer or strain gage is attached. The breaking strength and ultimate tensile strengths are calculated from the final load and max load respectively divided by the reduced cross-sectional area, A_r, where necking and fracture occurs. Variables and calculations used were as follows:

$$\mathrm{A_o} = \text{cross} - \text{sectional area (original)}$$

$$A_r = \text{reduced cross} - \text{sectional area}$$

$$P = \text{applied load}$$

$$P_f = \text{load at fracture}$$

$$P_{max} = \text{maximum load}$$

$$\Delta l = \text{measured elongation over 1in gage length}$$

$$\sigma_o = \frac{P}{A_o} = \text{stress}$$

$$\varepsilon = \frac{\Delta l}{1in} = \text{measured strain}$$

$$E = \frac{\sigma_o}{\varepsilon} = \text{modulus of elasticity}$$

$$\sigma_f = \frac{P_f}{A_r} = \text{fracture stress}$$

$$\sigma_u = \frac{P_u}{A_r} = \text{ultimate stress}$$

ASTM A931 details the procedure for the standard tension testing of wires and can be used as a guideline for testing of single wire. No standard is available for the testing of individual wires.

The strand from all three manufacturers was cut into 8in long bars and the center wire was extracted for this test. A 1.0in long segment of the center wire was reduced in cross section by 1mm using a lathe, shown in Figure 7.1. This was done to prevent the wire from breaking at the grips due to stress concentrations.

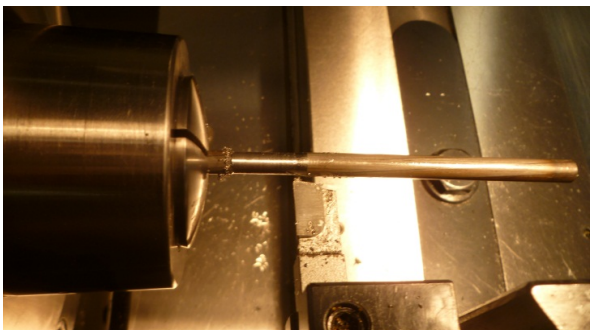

Figure-7. 1 Steel wire on lathe with reduced cross-section

7.3 Test Setup and Instrumentation

The test machine used was an MTS 20,000lb capacity tension/compression test console with hydraulic grips shown in Figure 7.2 (right). To measure strain in the elastic range a 1.0in gage-length extensometer was used for all test specimens. The extensometer was placed on the unmodified cross section of the wire, A_o. The location of the reduced cross-sectional area and specimen dimensions are shown in Figure 7.2 (left). The test was displacement controlled at a rate of 0.1in/min. After reaching nearly 70% of the expected capacity, the test was paused, the extensometer removed and the test was resumed until failure.

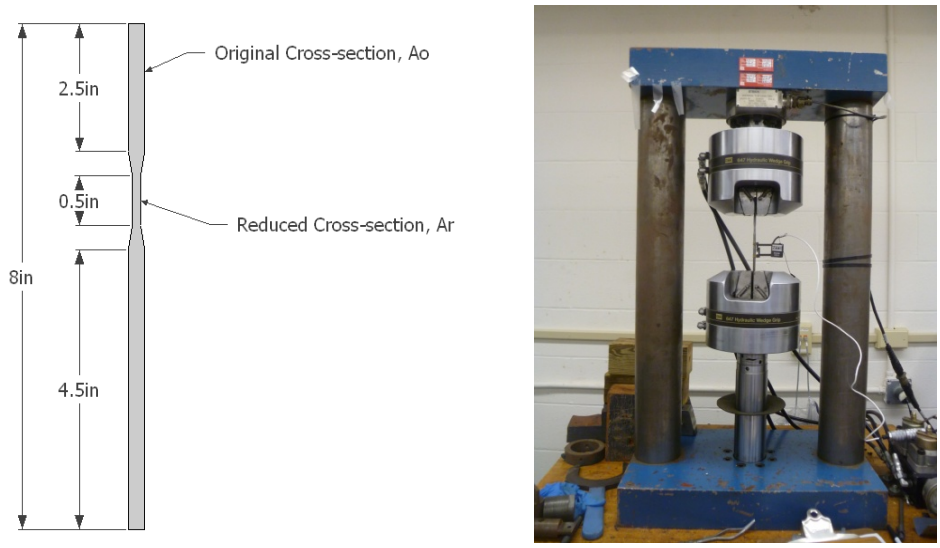

Figure-7. 2 Wire specimen dimensions (left) and MTS Console used for tension tests (right)

After viewing the results for the modulus of elasticity it was apparent that there existed some significant deviation of the experimental values from the theoretical 29,000ksi. An additional tension test was needed, using two strain gages in place of the extensometer to verify the possibility of developing bending moment. The gauges were attached to the area with the unmodified cross-section as shown in Figure 7.3. Data acquisition was not automated therefore the strain at the two gauges was manually recorded for several load values.

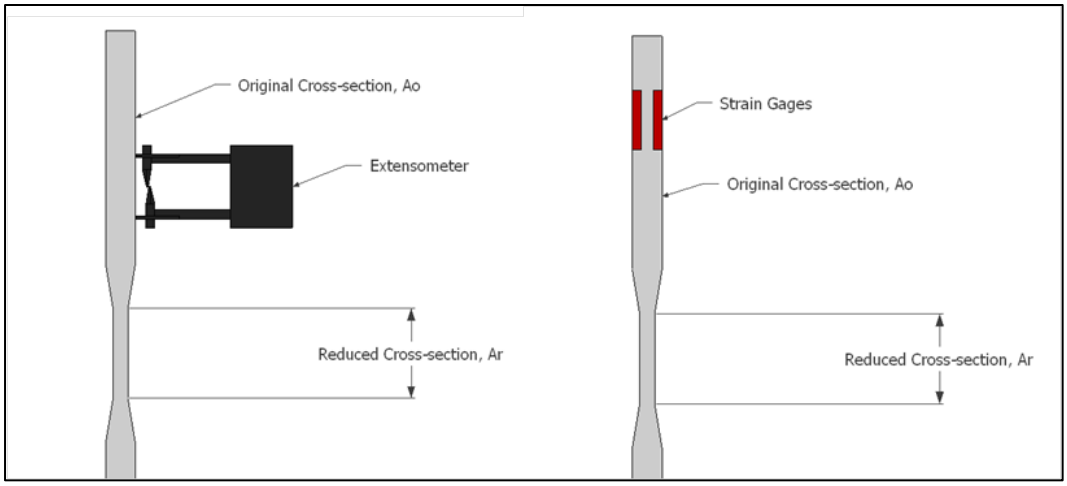

Figure-7. 3 Placement of extensometer (left) and strain gauges (right)

7.4 Results

A total of 18 test specimens were tested, with three repetitions for each variable. For each manufacturer, 3 un-heated and 3 heat-treated wires were tested. The ultimate tensile strength and the stress at fracture were directly obtained from the load values and the cross-sectional area while the modulus of elasticity was calculated from the stress-strain curve. The modulus of elasticity for prestressed reinforcement is reported by the manufacturer or determined by tests, whereas the modulus of elasticity of non-prestressed reinforcement shall be taken as 29,000ksi in keeping with ACI 318-11 Building Code section 8.5 [28]. However, the modulus values determined from these tension tests were inconsistent and highly deviate from the theoretical value for reinforcing steel. In the case of Steel-A, the only manufacturer for which modulus data was reported, it also deviates from the reported value. Table 7.1 summarizes the mechanical properties obtained for this test.

Table-7. 1 Tension Test Results

Steel-A Untreated			
Test No.	**Tensile Strength**	**Strength at Fracture**	**Modulus of Elasticity, E**
A-UT-01	313.3 ksi	275.5 ksi	32071 ksi
A-UT-02	294.7 ksi	258.4 ksi	32286 ksi
A-UT-03	294.6 ksi	240.3 ksi	34176 ksi
Average	**300.9 ksi**	**258.1 ksi**	**32844.3 ksi**
St. Dev.	10.7	17.6	1158.3

Steel-A Heat-Treated			
Test No.	**Tensile Strength**	**Strength at Fracture**	**Modulus of Elasticity, E**
A-HT-01	302.9 ksi	272.9 ksi	32450 ksi
A-HT-02	299.2 ksi	271.0 ksi	31587 ksi
A-HT-03	306.0 ksi	301.6 ksi	33080 ksi
Average	**302.7 ksi**	**281.8 ksi**	**32372.3 ksi**
St. Dev.	3.4	17.1	749.5

Steel-B Untreated			
Test No.	**Tensile Strength**	**Strength at Fracture**	**Modulus of Elasticity, E**
B-UT-01	300.2 ksi	263.8 ksi	32400 ksi
B-UT-02	297.4 ksi	244.1 ksi	33472 ksi
B-UT-03	300.1 ksi	259.4 ksi	33259 ksi
Average	**299.2 ksi**	**255.8 ksi**	**33043.7 ksi**
St. Dev.	1.6	10.3	567.5

Steel-B Heat-Treated			
Test No.	**Tensile Strength**	**Strength at Fracture**	**Modulus of Elasticity, E**
B-HT-01	298.2 ksi	278.1 ksi	35562 ksi
B-HT-02	296.5 ksi	264.3 ksi	37465 ksi
B-HT-03	300.9 ksi	285.8 ksi	32974 ksi
Average	**298.5 ksi**	**276.0 ksi**	**35333.7 ksi**
St. Dev.	2.2	10.9	2254.2

Steel-C Wire Untreated			
Test No.	**Tensile Strength**	**Strength at Fracture**	**Modulus of Elasticity, E**
C-UT-01	305.6 ksi	276.4 ksi	33400 ksi
C-UT-02	312.9 ksi	279.8 ksi	36959 ksi
C-UT-03	321.9 ksi	266.8 ksi	34294 ksi
Average	**313.5 ksi**	**274.3**	**34884.3 ksi**
St. Dev.	8.2	6.7	1851.5

Steel-C Heat-Treated			
Test No.	**Tensile Strength**	**Strength at Fracture**	**Modulus of Elasticity, E**
C-HT-01	302.3 ksi	293.1 ksi	34510 ksi
C-HT-02	304.6 ksi	286.1 ksi	33258 ksi
C-HT-03	305.8 ksi	295.4 ksi	28034 ksi
Average	**304.2 ksi**	**291.5 ksi**	**31934.0 ksi**
St. Dev.	1.8	4.8	3435.0

The result for the tension test using strain gauges is shown in Table 7.2. The values presented in this table are only for a Steel-B wire that has not been heated. The modulus of elasticity obtained from this test is the same as the average obtained for the same sample type using the extensometer. From the strain values the presence of bending can be corroborated. Refer to the Appendix Section-D for the strain values.

Table-7. 2 Results from tension test using strain gauges

Steel-B Untreated-Strain Gage			
Test No.	**Tensile Strength**	**Strength at Fracture**	**Modulus of Elasticity, E**
B-UT-SG	307.2 ksi	277.8 ksi	32896 ksi

Chapter 8: Discussion and Recommendations

8.1 Discussion and Conclusions

The quality of the coating is affected largely in part by the condition of the substrate, in this case the carbon steel surface. Presence of a layer of particles of calcium oxides and carbonates, resulting from the treatment of the strands with calcium stearate in the manufacturing process, causes the zirconia sol to gel on the surface of the wire during dip coating. The resulting coating is made of a thick layer of powder; this layer is loosely held to the metal and provides very small protection from pitting corrosion.

When wires are treated to remove some of the calcium left behind by lubricants, iron oxide that is left in its place combined with either zirconia or titania, provide good coating adhesion and corrosion protection. Treating the wires with either acid solutions of HNO_3 or HCl or a basic solution of 1:4 ratio of H_2O_2 and 3M NaOH improves the nature of the oxide films and the protection of these coatings against corrosion. The basic treatment was the most effective.

Wires coated with zirconia render more positive critical pitting corrosion potentials than the ones coated with titania, meaning that the former oxide coatings provides a better protection from corrosion than the later. Zirconia was then used for all electrochemical and structural testing.

An improvement on the corrosion resistance of a material is analogous to a change in the critical pitting corrosion potential, E_{pit}, of the material to a more positive value. More positive pitting potential values were recorded for coated samples relative to bare wire, regardless of the manufacturer. The wires that achieved the most positive values of E_{pit} belong to

manufacturer American Spring Wire, designated as Steel-C. The average pitting potential of the coated samples was about 500mV, which represents a 600mV increase from the pitting potential of bare wire. The E_{pit} of Steel-A increased by 400mV and of Steel-B by 100mV. This indicates that the performance of the coating is dependent on the surface finish.

Subjecting the wires to tension stress, releasing the tension and then performing the anodic polarization measurements led to a different outcome. Stretched-bare wire outperformed the coated wires that had been stretched and also those that had not been stretched. This result was surprising since the effect of pitting should be intensified by stress. SEM imaging of coated and stretched wires show a large roughening of the surface upon stretching, although they also show an almost integral coating with a few more cracks in some cases. However, cross-section images of uncoated wires, both un-stretched and stretched, clearly indicate stretching breaks the outer layer of the wire. Thus, it seems that the zirconia coating is covering this region, but the adhesion to the surface of the wire is very small, lowering its effectiveness as corrosion protection.

Test results from bond testing can be interpreted in two ways. As opposed to the NASP Test and other pull-out tests being researched, this small-scale test uses only one single wire as a test specimen, embedded in concrete mortar. The bond is mainly provided by chemical adhesion and friction since mechanical interlock is negligible. In this case, the data should be examined more closely. By examining the bond strength values at 0.1in slip, the data are inconclusive. For one manufacturer, Sumiden, the coating increases the steel-concrete bond, while for Insteel and American Spring Wire, the pull-out capacity is less than the bare wire. On the other hand, if the maximum values are analyzed, they show a different tendency. The

maximum load value occurs when the wire first starts to slip, in other words, when it is no longer bonded to the mortar. After this initial debonding, friction is the predominant source of bond. In this case, coated test specimens for all three manufactures show an increase of two times the maximum load of bare wires.

When applying these coatings it is important to think of any adhesion they might add or detract from the bond to concrete. The maximum values of pull-out force should be more indicative of adhesion to the mortar. From the small-scale pull-out test it was concluded that the coating does significantly improve adhesion to concrete, which will benefit the bond stress.

Tension tests performed on heat-treated wires and wires in an "as-received" condition revealed that the heat-treatment used in the sintering process for coating the wires did not have any negative effects on the mechanical properties of the steel.

Fracture and ultimate tensile loads remained unaltered. As for the modulus of elasticity, it was expected to decrease should any phase changes start to occur. The average value for all sets of test-specimens was beyond the accepted value of 29,000ksi for reinforcing steel. For prestressing strand the value is reported by the manufacturer [28]. However, the elastic modulus obtained from testing is about 15% higher than the value reported by the producer. The modulus of elasticity for the reel of strand provided by Sumiden was reported as 28,600ksi.

It should be noted that the setup had some flaws. The MTS system used flat hydraulic grips given that no round grips of the appropriate diameter were available. This creates stress

concentrations and alignment errors. The diameters of the wires were small (5mm and 4mm) and while the wires used for this test were all king wires, they are not perfectly straight. These two factors augment the possibility of bending developing in the test specimen.

By using strain gages on an un-treated wire from Insteel the presence of bending was confirmed. As much as an average of 25% of bending strain with respect to axial strain can be observed in the elastic range. The value for the modulus of elasticity found by this method was the same as that found using an extensometer. However, the elastic modulus obtained from testing may still be used to compare changes in this parameter caused by the heat-treatment. No significant changes in ultimate tensile and fracture strengths or modulus of elasticity were observed. Therefore, the heat treatment should not affect the mechanical properties of the strand and the coating procedure is viable for this material.

In summary, the coatings do add some corrosion resistance to the steel wire, provided that the surface is adequately treated prior to coating. Upon stretching and then releasing the tension load completely, the performance of the coating, in terms of change in pitting corrosion potential, is reduced by as much as 95%. This however is not an in situ test and in practice the tension stress would not be completely reduced to zero. This should be investigated more closely. The coatings do add some adhesion to the mortar as observed by the bond tests results. Finally the coating process does not affect the mechanical and material properties of the carbon steel. Therefore, the coatings are viable as corrosion protection method for structural carbon steel. However, as for their use in prestressing applications, more testing should be done to study their elasticity and behavior upon stretching.

8.2 Recommendations

Electrochemical testing should be complemented with Electrochemical Impedance Spectroscopy (EIS) studies in order to have a better understanding of the processes occurring at the electrode (steel) interface and the type of protection offered by the coatings. More research should be focused on the steel surface characterization and pretreatment. The effectiveness of the coating is sensitive to the condition of the substrate and a significant amount of research time should be allotted to this subject. Also, further testing should include coating the whole strand and testing the coating's resistance to abrasion as well as its electrochemical behavior. Electrochemical testing of coated strands embedded in concrete should also be considered, with careful consideration to variables such as environmental pH, curing temperature and permeability of the concrete.

Electrochemical tests should be performed while the wire or strand is subjected to some tension as it would be on a prestressed concrete girder. If electrochemical testing and SEM photos cannot be taken of stretched wire, one should consider removing the stress at a very slow rate so as to avoid fast, drastic changes in microstructure. Finally, in terms of its effect on the steel-concrete bond, a full NASP bond test should be performed and compared to the literature.

References

[1] C. K. Nmai and D. M. Suchorski, “Reinforcement for Concrete— Materials and Applications,” American Concrete Institute, ACI Education Bulletin E2-00, 2000.[1] C. K. Nmai and D. M. Suchorski, “Reinforcement for Concrete— Materials and Applications,” American Concrete Institute, ACI Education Bulletin E2-00, 2000.

[2] G. H. Koch, M. P. H. Brongers, N. G. Thompson, Y. P. Virmani, and J. H. Payer, “Corrosion Costs and Preventive Strategies in the United States,” National Association of Corrosion Engineers (NACE), Publication No. FHWA-RD-01-156.

[3] J. T. Wolsiefer, “Silica Fume Concrete: a Solution to Steel Reinforcement Corrosion in Concrete,” presented at the Second CANMET/ACI International Conference on Durability of Concrete, Montreal, Canada, 1991.

[4] K. Brosseau, “Cathodic Protection of Reinforced Concrete Bridge Elements: A State-of-the-Art Report,” Strategic Highway Research Program National Research Counsil, SHRP-S-337, 1993.

[5] J. L. Smith and Y. P. Virmani, “Materials and Methods for Corrosion Control of Reinforced and Prestressed Concrete Structures in New Construction,” Final Report FHWA-RD-00-081.

[6] K. . C. Clear, “Effectiveness of Epoxy-coated Reinforcing Steel,” Concrete International, vol. 14, no. 5, pp. 58, 60–2, May 1992.

[7] C. Alonso, M. Castellote, and C. Andrade, “Chloride Threshold Dependence of Pitting Potential of Reinforcements,” Electrochimica Acta, vol. 47, 2002.

[8] D. Stark, "Influence of Design and Materials on Corrosion Resistance of Steel in Concrete," Research and Development Bulletin R098.01T, 1989.

[9] M. Hurley and J. R. Scully, "Chloride Threshold Levels in Clad 316L and Solid 316LN Stainless Steel Rebar," NACE Corrosion, 02224, 2002.

[10] J. Zemajtis, R. E. Weyers, M. M. Sprinkel, and W. T. McKeel, "Epoxy-Coated Reinforcement - A Historical Performance Review," Virginia Transportation Research Counsil, Interim Report VTRC 97-IR1, Sep. 1996.

[11] G. G. Miller, J. Kepler, and D. Darwin, "Effect of Epoxy Coating Thickness on Bond Strength of Reinforcing Bars," ACI Structural Journal, Jun. 2003.

[12] W. A. Pyc, "Performance Evaluation of Epoxy- Coated Reinforcing Steel and Corrosion Inhibitors in a Simulated Concrete Pore Water Solution," Virginia Polytechnic Institute and State University, 1997.

[13] W. A. Pyc, "Field Performance of Epoxy-Coated Reinforcing Steel in Virginia Bridge Decks," Virginia Polytechnic Institute and State University, 1998.

[14] J. A. Pincheira, A. A. Aramayo, and K. S. Kim, "Corrosion Protection Performance of Epoxy-Coated Reinforcing Bars," University of Wisconsin-Madison, Final Report MN/RC 2008-47, Sep. 2008.

[15] R. E. Weyers, M. M. Sprinkel, and M. C. Brown, "Summary Report on the Performance of Epoxy-Coated Reinforcing Steel in Virginia," Virginia Transportation Research Counsil, VTRC 06-R29, Jun. 2006.

[16] R. Park and T. Paulay, Reinforced Concrete Structures. John Wiley and Sons, 1975.

[17] O. A. Kayyali and S. R. Yeomans, “Bond and slip of coated reinforcement in concrete,” Construction and Building Materials, vol. 9, no. 4, pp. 219–226, 1995.

[18] M. Haskett, D. J. Oehlers, and M. S. Mohamed Ali, “Local and global bond characteristics of steel reinforcing bars,” Engineering Structures, vol. 30, no. 2, pp. 376–383, Feb. 2008.

[19] B. W. Russell, “NASP Round IV Strand Bond Testing,” The North American Strand Producers, Final Report.

[20] D. J.R., Corrosion: Understanding the Basics. ASM International, 2000.

[21] E. McCafferty, Introduction to Corrosion Science. 2010.

[22] A. E. N. Osborn, J. S. Lawler, and J. D. Connolly, “Acceptance Tests for Surface Characteristics of Steel Strands in Prestressed Concrete,” Transportation Research Board, NCHRP 621, 2008.

[23] R. Hudson, “The Sherwin Williams Company Industrial and Marine Coatings,” Update of a DTI Publication Firts Issued in 1982.

[24] S. Tang, O.-J. Kwon, N. Lu, and H.-S. Choi, “Surface and Coating Technology,” 2005.

[25] M. Anderson, I. Tejedor, and C. Ole, “Metal Substrates Including Metal Oxide Nanoporous Thin Films and Methods of Making the Same.”

[26] Q. Xu, “Physical-chemical Factors Affecting the Synthesis and Characteristics of Transition Metal Oxide Membranes,” University of Wisconsin - Madison, 1991.

[27] K. B. Oldham and J. C. Myland, Fundamentals of Electro Chemical Science. Academic Press, Inc., 1994.

[28] ACI Committee 318, Building Code Requirements for Structural Concrete, ACI 318-11. Amercian Concrete Institute, 2011.

Appendix

Section – A

Critical Pitting Corrosion Potentials – Coating Quality Testing

Table-A. 1 Critical Pitting Corrosion Potentials

Sumiden-Sample ID	E_{pit} [mV]
A-steel270-uncoated-washed-01	-120
A-steel270-uncoated-washed-02	-130
A-steel270-uncoated-washed-03	-180
A-steel270-ZrO2-washed-4L-01	40
A-steel270-ZrO2-washed-4L-02	-200
A-steel270-ZrO2-washed-4L-03	-240
A-steel270-ZrO2-washed-8L-01	-50
A-steel270-ZrO2-washed-8L-02	-100
A-steel270-ZrO2-washed-8L-03	-140
A-steel270-ZrO2-HNO3+350C-8L-01	-140
A-steel270-ZrO2-H2O2+HNO3-8L-01	40
A-steel270-ZrO2-H2O2+HNO3-8L-02	-70
A-steel270-ZrO2-450Csintering-8L-01	-130
A-steel270-ZrO2-450Csintering-8L-02	-130
A-steel270-ZrO2-H2O2-8L-01	40
A-steel270-ZrO2-H2O2-12L-01	310
A-steel270-ZrO2-H2O2-12L-02	200
A-steel270-ZrO2-H2O2-12L-03	250
A-steel270-TiO2+ZrO2-H2O2-1hr-01	0
A-steel270-TiO2-H2O2-1hr-01	0
A-steel270-TiO2-H2O2-30min-01	-240
A-steel270-ZrO2-Polish-8L-01	350
A-steel270-ZrO2-Polish+Sanded-4L-01	100
A-steel270-ZrO2-Polish+Sanded-8L-01	110
A-steel270-ZrO2-pH2.95-H2O2-8L-01	40
A-steel270-ZrO2-pH2.59-H2O2-8L-01	20
A-steel270-ZrO2-pH2.95-HCl-8L-01	-110
A-steel270-ZrO2-pH2.59-HCl-8L-01	-100
A-wire-ZrO2-H2O2-8L-01	-20
A-wire-ZrO2-H2O2-8L-02	-20

Section – B

Critical Pitting Corrosion Potentials – Corrosion Protection Testing

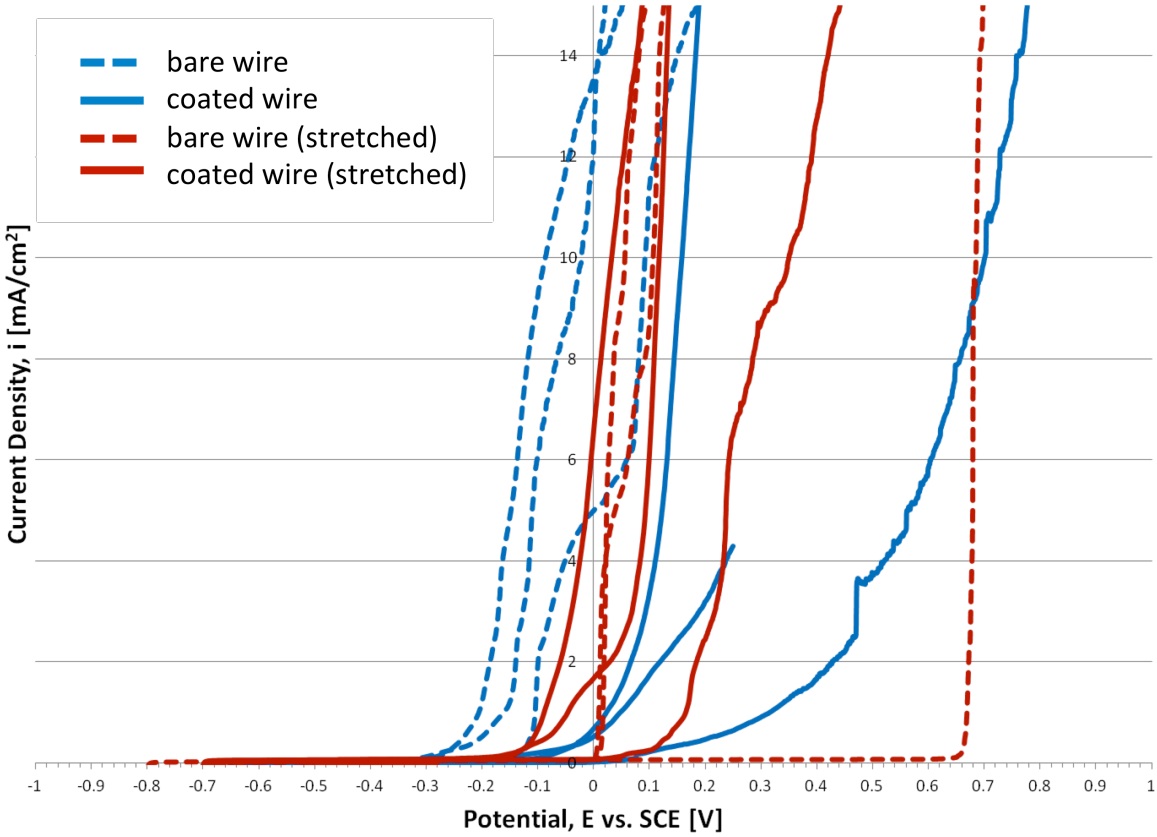

Figure-B. 1 Polarization Curves for Steel-A

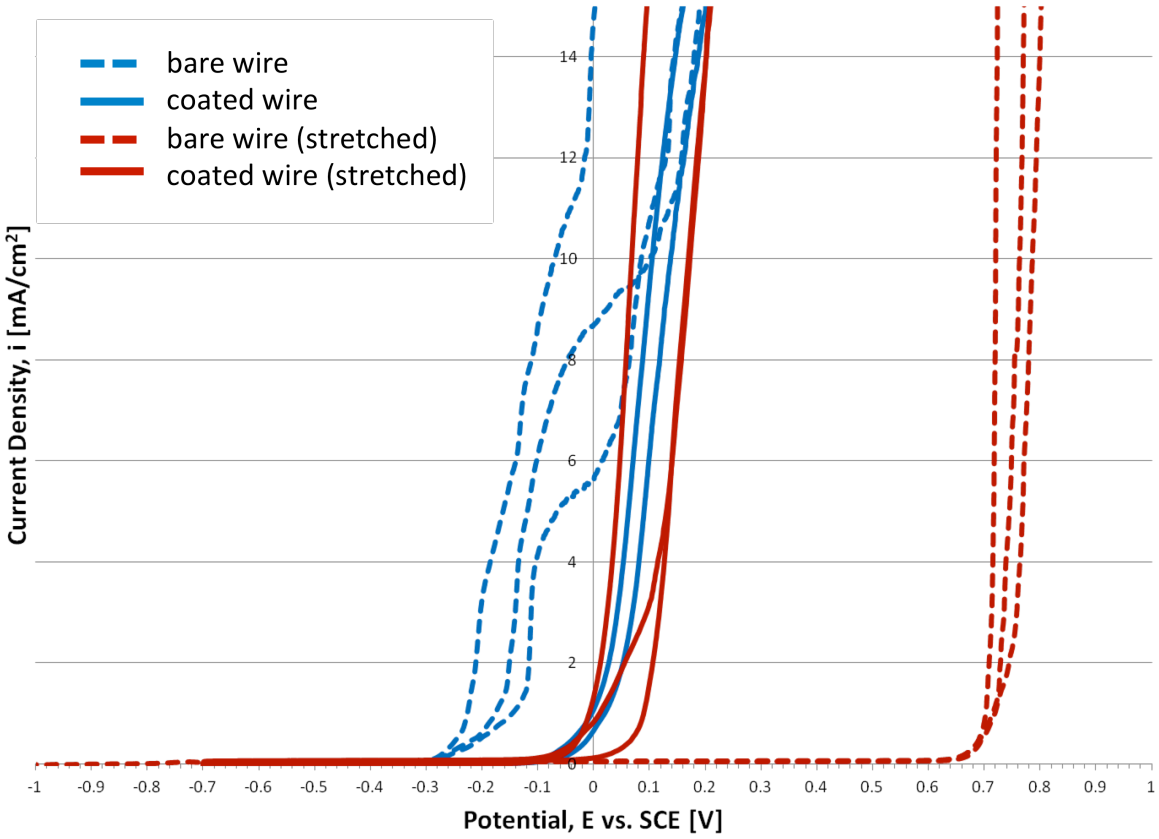

Figure-B. 2 Polarization Curves for Steel-B

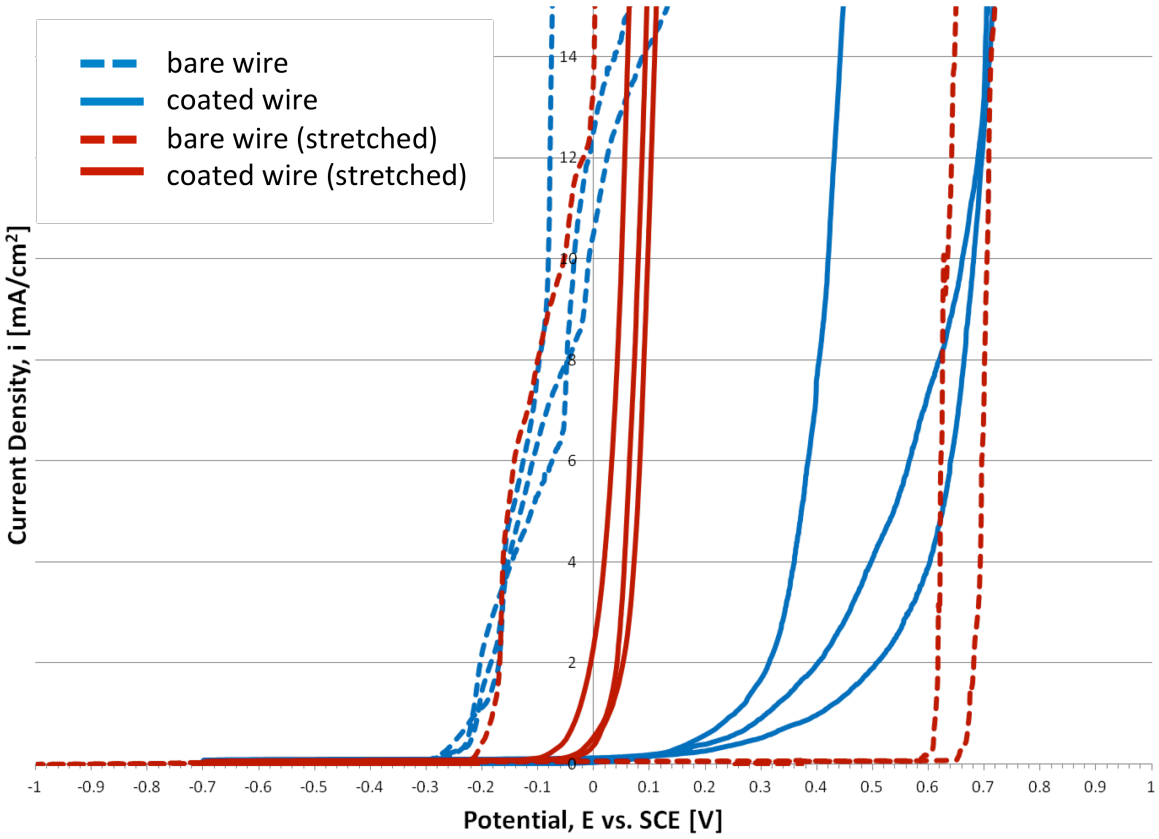

Figure-B. 3 Polarization Curves for Steel-A

Section – C

Pull-out Test Plots

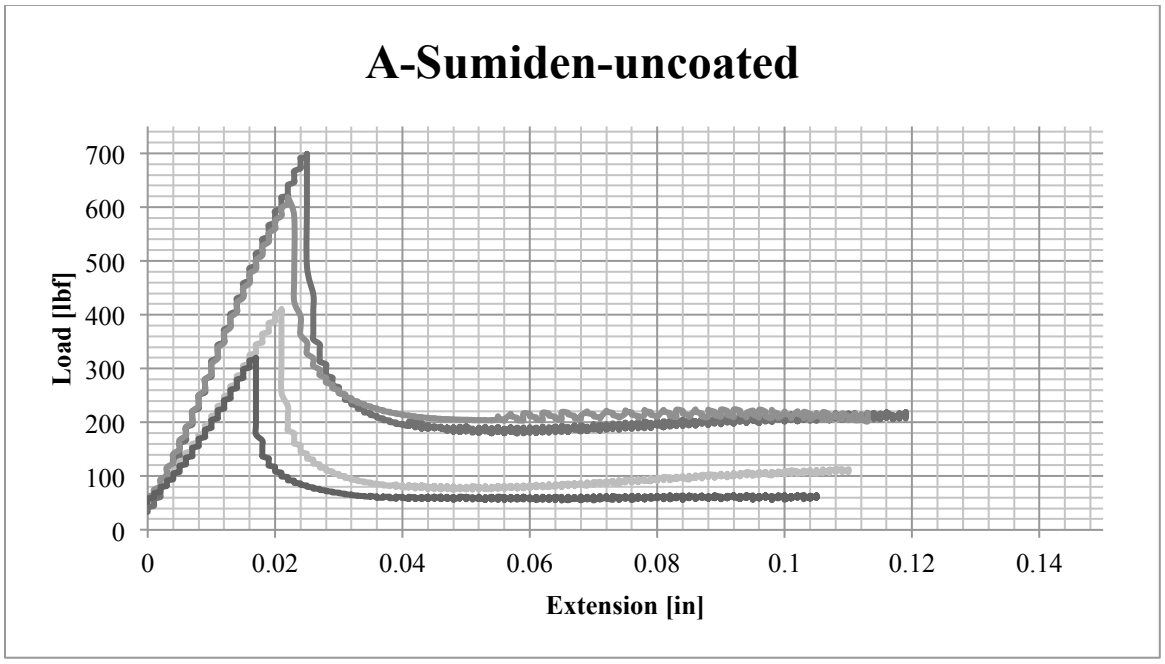

Figure-C. 1 Pull-Out Tests Plot - Steel-A: Uncoated

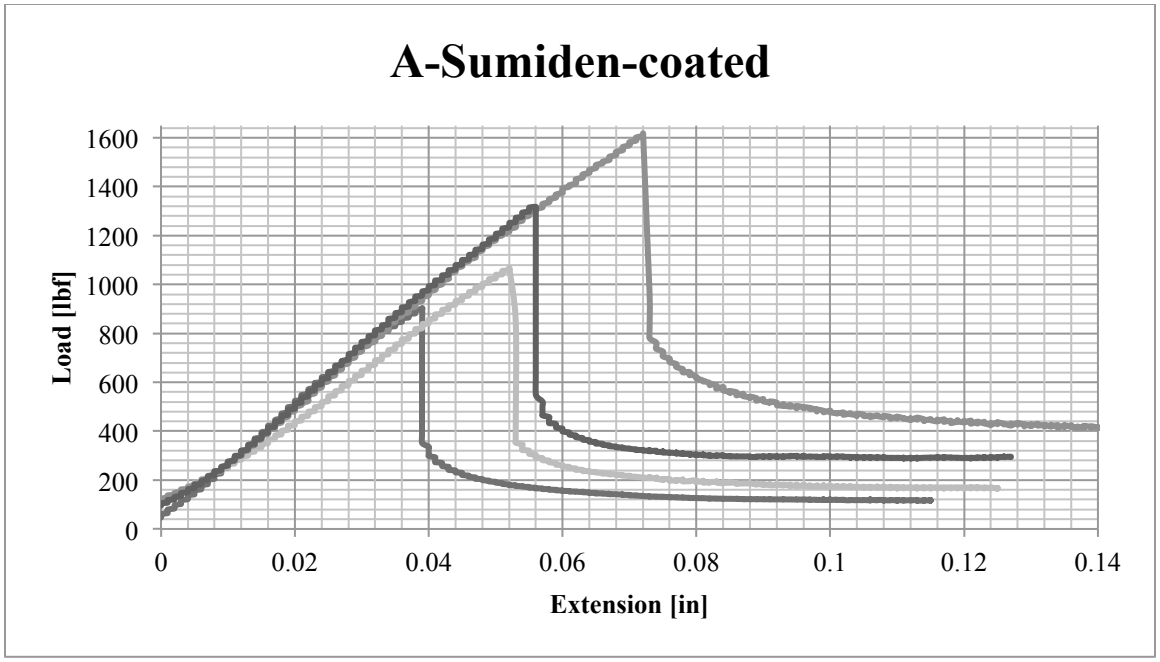

Figure-C. 2 Pull-Out Tests Plot - Steel-A: Coated

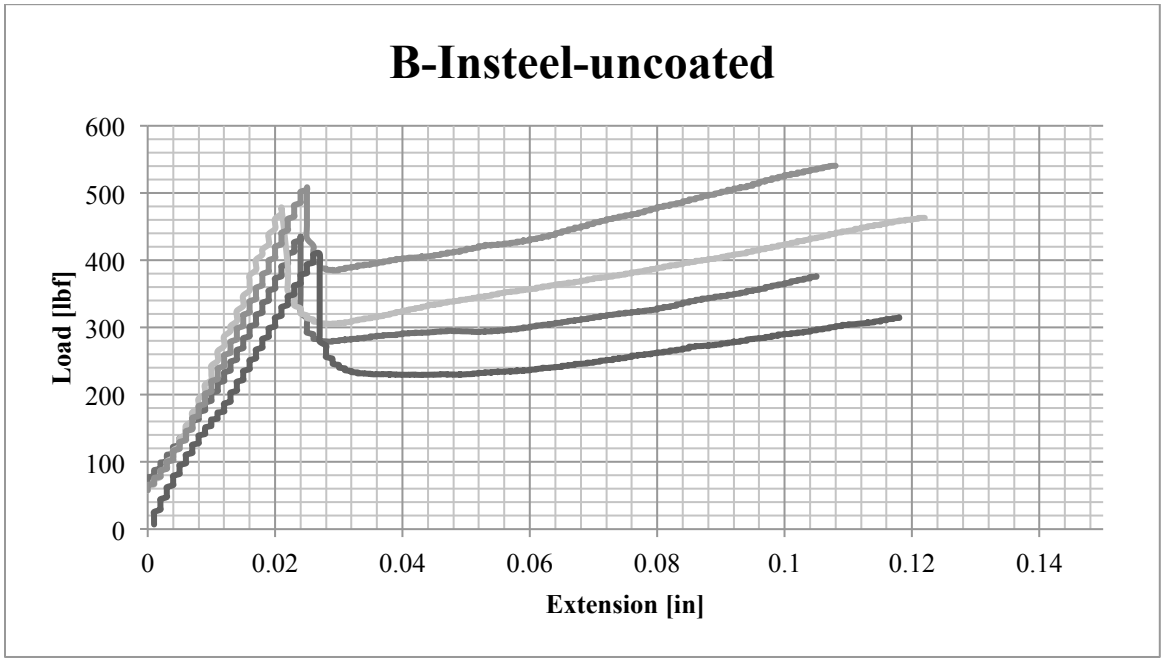

Figure-C. 3 Pull-Out Tests Plot - Steel-B: Uncoated

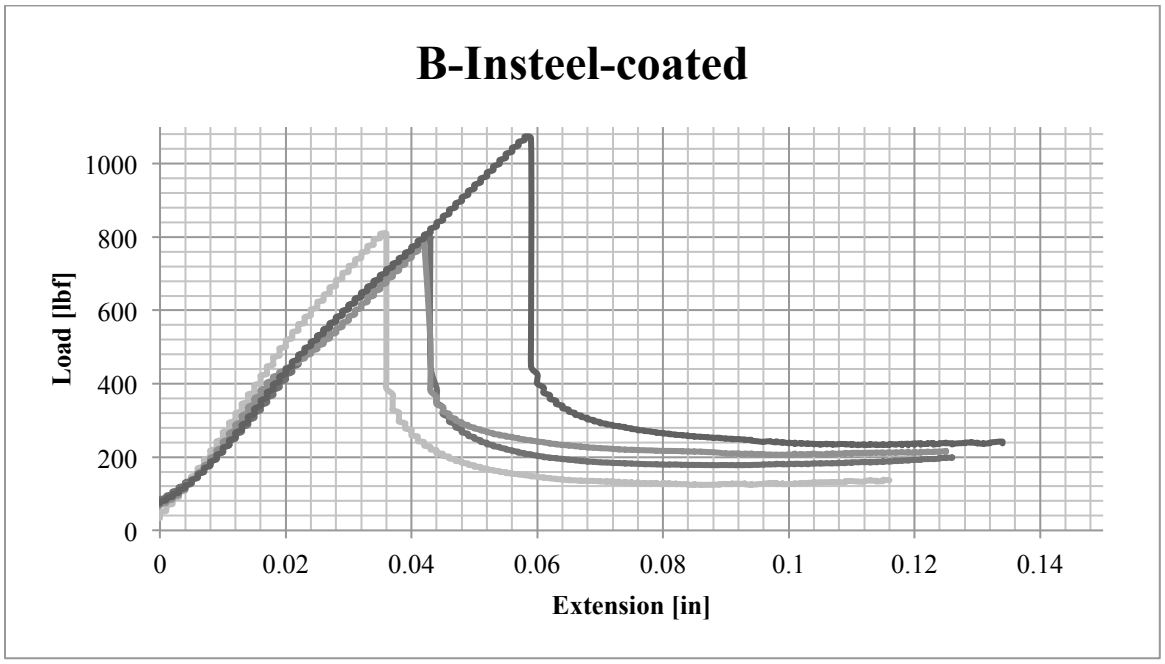

Figure-C. 4 Pull-Out Tests Plot - Steel-B: Coated

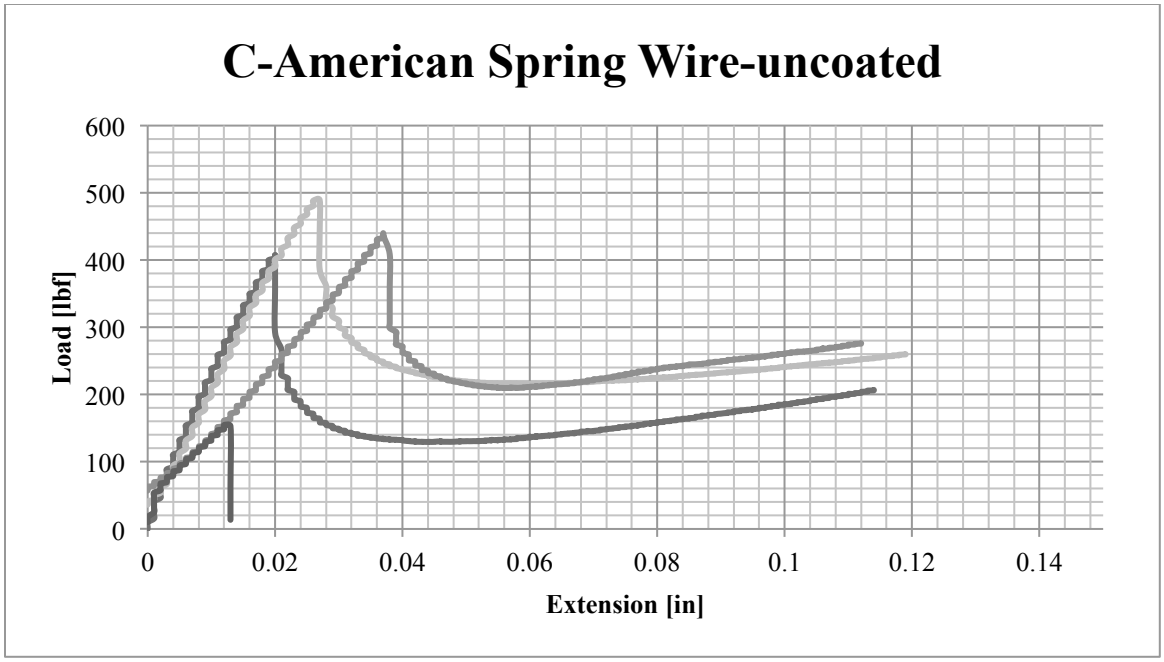

Figure-C. 5 Pull-Out Tests Plot - Steel-C: Uncoated

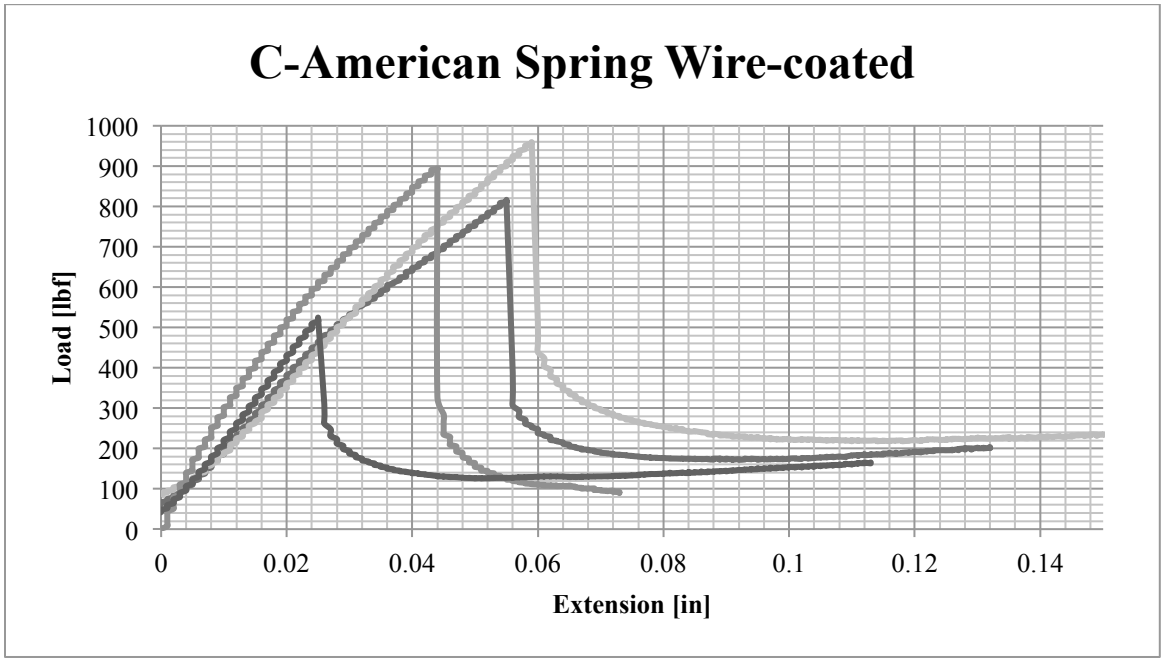

Figure-C. 6 Pull-Out Tests Plot - Steel-C: Coated

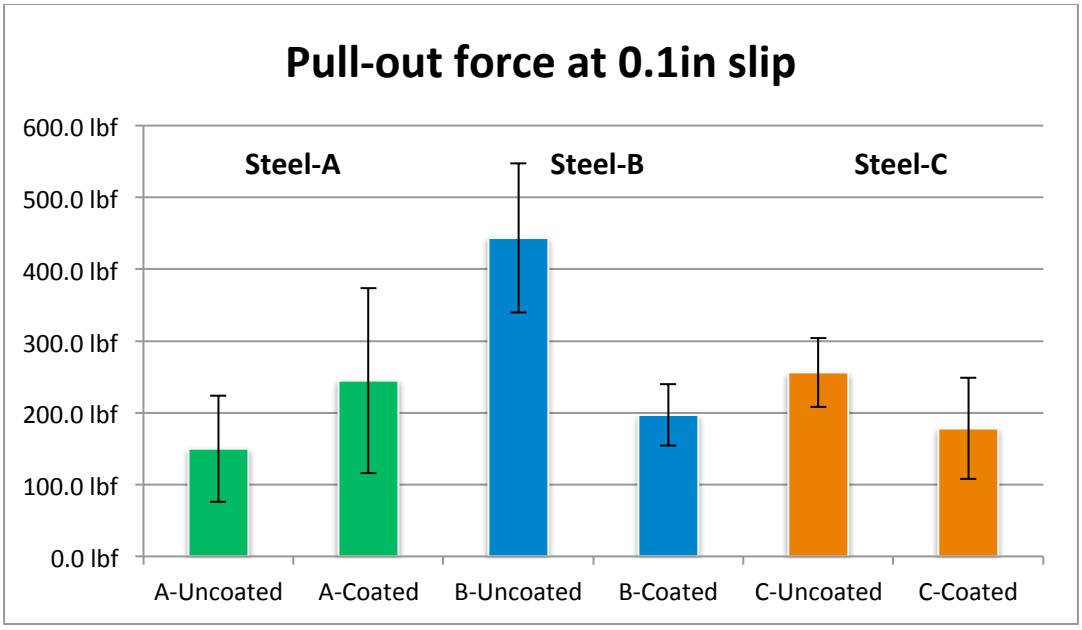

Figure-C. 7 Pull-out force at 0.1in slip for bare and coated wires for all three manufacturers: Steel-A: green, Steel-B: blue, Steel-C: orange. The error bars show the standard deviation for 95% probability. Values for uncoated and coated sample are not statistically different in this case.

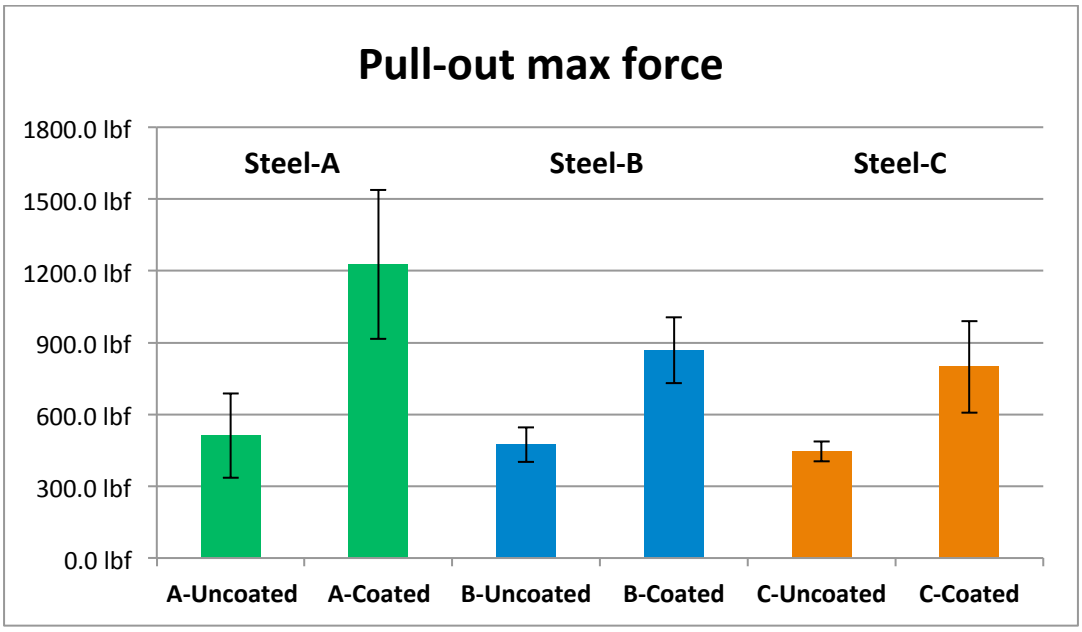

Figure-C. 8 Pull-out max force or force at first slip for bare and coated wires for all three manufacturers: Steel-A: green, Steel-B: blue, Steel-C: orange. The error bars show the standard deviation for 95% probability. Values for uncoated and coated sample are statistically different in this case.

Section – D

Tension Test on Individual Wires

Table-D. 1 Load and Strain for Tension Test on Steel-B (no heat treatment) with Strain Gauges

Rate	0.005	in/min
Load (lbf)	**Strain1 x10^{-6}**	**Strain2 x10^{-6}**
-470	350	-350
-337	450	-250
-234	590	-140
296	1150	312
437	1300	450
563	1450	530
732	1600	720
859	1750	840
1023	1900	975
1146	2050	1094
1341	2250	1288
1453	2350	1390
1598	2500	1515
1733	2650	1860
1890	2800	1425
2078	3000	1950
2285	3200	2142
2477	3400	2333
2671	3600	2621
2879	3800	2642
3056	4000	2895
3254	4200	3090
3459	4400	3294
3880	4800	3639

Load (lbf)	**Strain1 x10^{-6}**	**Strain2 x10^{-6}**
4051	5000	3872
4259	5200	4077
4452	5400	4295
4646	5600	4484
4847	5800	4675
5027	6000	4874
5222	6200	5088
5431	6400	5145
5627	6600	5507
5814	6800	5714
5953	6950	5866
6008	7000	5922
6109	7100	6030
6202	7200	6133
6298	7300	6242
6402	7400	6356
6490	7500	6459
6403	7430	6380
6348	7370	6334
6271	7300	6258
6185	7200	6173
6067	7100	6066
5975	7000	5960
5868	6900	5868

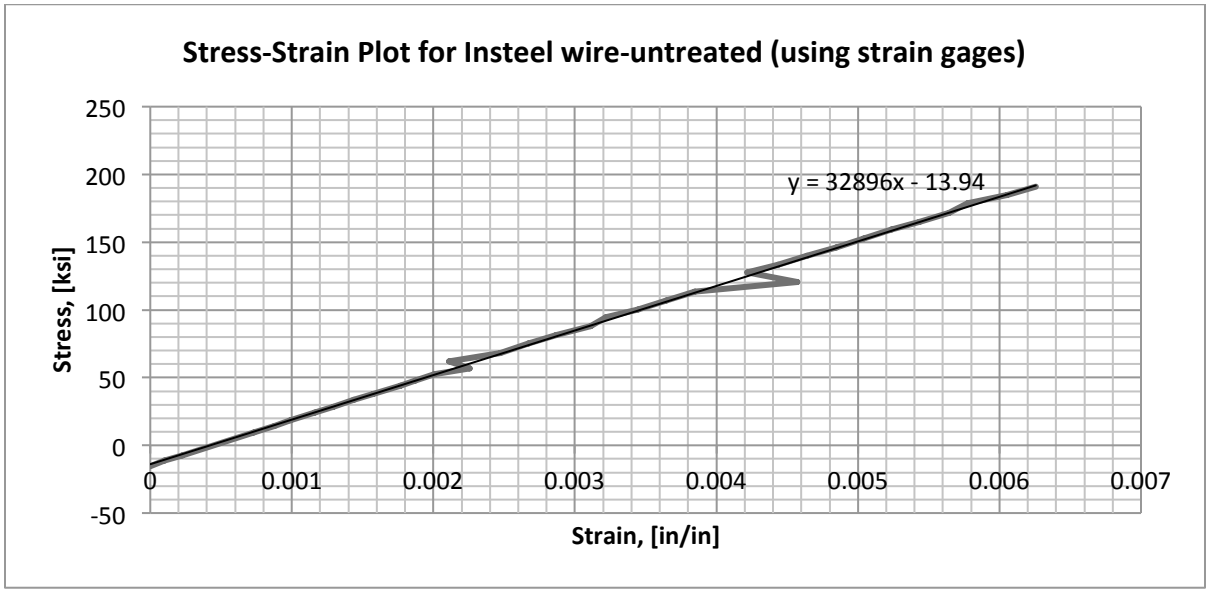

Figure-D. 1 Stress-Strain Curve for Insteel Wire (With Strain Gauges)

CFIRE

University of Wisconsin-Madison
Department of Civil and Environmental Engineering
1410 Engineering Drive, Room 270
Madison, WI 53706
Phone: 608-263-3175
Fax: 608-263-2512
cfire.wistrans.org